

**STATE OF NEVADA - FUNDED RESEARCH**

**INTRAVAL MODELING CONCLUSIONS  
ADDRESSING NON-UNIQUE SOLUTIONS**

BY

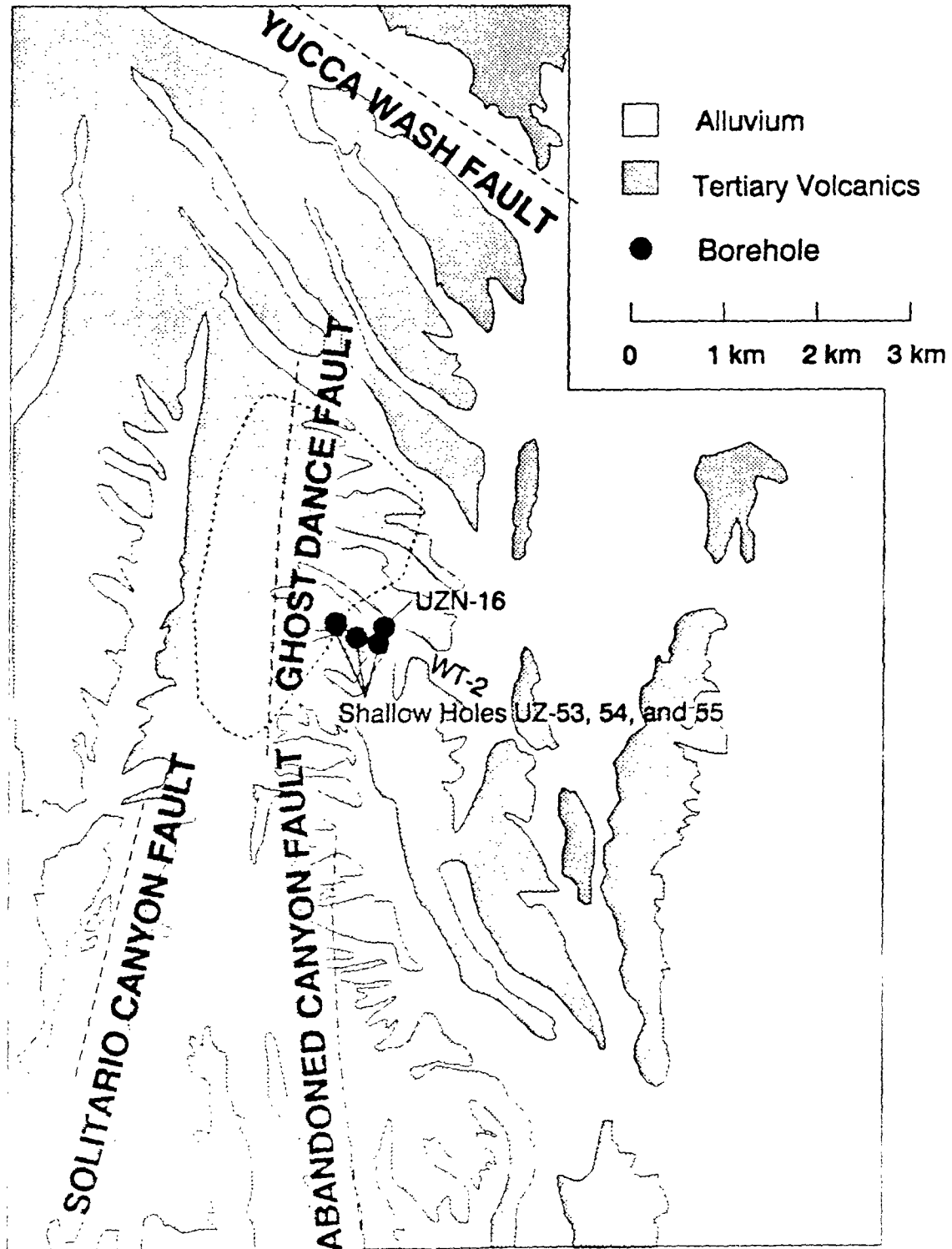
LINDA LEHMAN, PRESIDENT  
L. LEHMAN & ASSOCIATES, INC.  
1103 W. BURNSVILLE PARKWAY  
SUITE 209  
BURNSVILLE, MN 55337  
(612) 894-0357

# **UNSATURATED ZONE TEST CASE**

## **PROBLEM DEFINITION**

- 1. CALIBRATE AGAINST WATER CONTENT PROFILES IN SHALLOW BOREHOLES UZN-53, UZN-54 AND UZN-55.**
- 2. PERFORM A BLIND PREDICTION OF THE WATER CONTENT PROFILES IN YET TO BE DRILLED BOREHOLE UZ-16 (SOME DATA WERE TO BE WITHHELD).**

# Location of Boreholes Used for Modeling Study



L. Lehman & Associates, Inc.

1993

## MEASURED PROPERTIES

Particle Density	$(\rho_s)$
Bulk Density	$(\rho_b)$
Porosity	$n$
Saturated Conductivity	$K_{sat}$
Water Retention	$S(\psi)$
Water Content	$\theta_{holes}$

## CALCULATED PROPERTIES

Relative Conductivity	$K_{rel}$
Saturated Conductivity	$K_{sat}$
Matric Suction	$\psi$
Water Content	$\theta$

## **DATA SET**

The data set for the Yucca Mountain test case is derived from a combination of samples collected in field transects along outcrops and core specimens from several boreholes in the area. These data were used to assemble a vertical composite transect representing all the units between the surface and the water table. The sources of information consist of:

### **OUTCROP DATA**

#### **UZ-6 Transect**

A vertical transect starting at the Tiva Canyon upper cliff unit near the UZ-6s borehole extending downward 1032 ft (313 m) through the Topopah Spring welded lower lithophysal unit at the Solitario Canyon Fault.

#### **Busted Butte Transect**

Vertical transect starting at the Topopah Spring basal vitrophyre on the east side of Busted Butte and extending 43 ft (13 m) upward through the base of the Topopah Spring nonwelded unit.

#### **Calico Hills Transect**

A vertical transect located north of Prow Pass, starting in the Prow Pass unit and extending 333 ft (101 m) upward through the Calico Hills zeolitized unit.

### **BOREHOLE DATA**

#### **USW GU-3 Borehole**

Borehole located at the south end of Yucca Crest. Consists of core data from depths between 1260 and 1900 ft (382 to 576 m) and includes the shardy base of the Topopah Spring unit through the nonwelded vitric Calico Hills unit and the nonwelded and partially welded Prow Pass unit.

#### **N53, N54 and N55 Boreholes** (Shallow wells)

Boreholes located in the WT-2 wash. Consists of core data from the surface to the top of the Topopah Spring and includes welded, moderately welded vitric and nonwelded portions of the Tiva Canyon unit, the Bedded/Nonwelded unit, and the nonwelded and welded caprock of the Tiva Canyon unit.

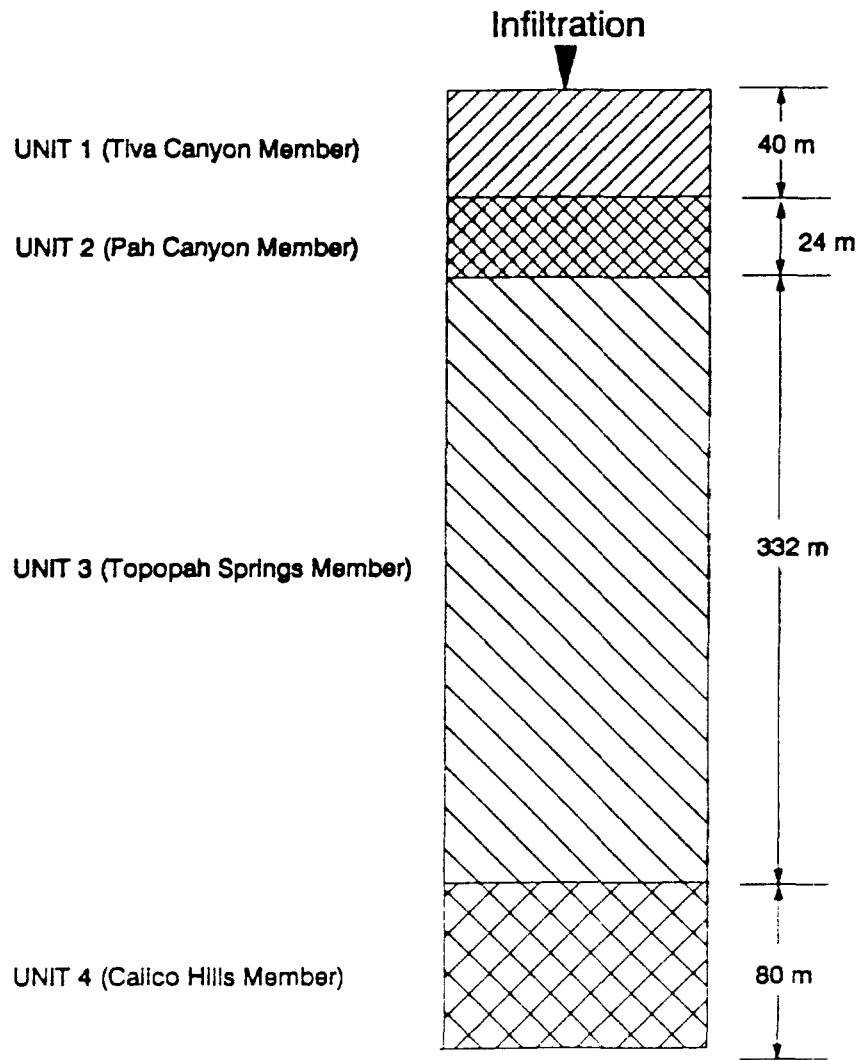
**Important Modeled Processes in L. Lehman & Associates Yucca Mountain  
Unsaturated Zone Models.**

PROCESS	MODELS	BASIS	DATA SOURCES
Zonation of hydrologic properties	1-D 2-D DFR FRACTURE	Geologic coring and mapping	<ul style="list-style-type: none"> <li>• Working group data (USGS)</li> <li>• Hole data from UZN holes 53, 54 and 55</li> </ul>
Matrix flow	1-D 2-D DFR FRACTURE	Predominance of wet porous media	<ul style="list-style-type: none"> <li>• Working group data (USGS)</li> <li>• Hole data from UZN holes 53, 54 and 55</li> <li>• Tyler, (1987)</li> </ul>
Fracture flow	FRACTURE	<ul style="list-style-type: none"> <li>• High fracture densities</li> <li>• Wet fractures observed in drilling UZN-54 &amp; 55</li> <li>• Lehman (1992)</li> <li>• Montazer &amp; Wilson (1984)</li> </ul>	<ul style="list-style-type: none"> <li>• Spengler &amp; Chornack (1984)</li> <li>• Wang &amp; Narasimhan (1985)</li> </ul>
Fracture/matrix interaction	FRACTURE	<ul style="list-style-type: none"> <li>• Existence of fracture coatings</li> <li>• Existence of transient infiltration</li> </ul>	Thoma et al. (1992)
Evaporation	DFR FRACTURE	<ul style="list-style-type: none"> <li>• High solar radiation in desert terrain</li> <li>• DFR model of Nieber et al. (1993)</li> </ul>	U.S. Weather Service
Focused infiltration	2-D DFR FRACTURE	<ul style="list-style-type: none"> <li>• Topography</li> <li>• Large conductivity contrasts in materials</li> </ul>	<ul style="list-style-type: none"> <li>• Nieber et al. (1993)</li> <li>• Harrill et al. (1988)</li> <li>• Hokett et al. (1991)</li> </ul>
Transient infiltration	1-D 2-D DFR FRACTURE	Long time frame with high probability of climate change	Spaulding (1983)

**1-Dimensional Simulation Features.**

Simulation Designator	# of Model Elements	# of Hydrologic Units	Infiltration Model (mm/yr)	Saturated Conductivity Model (per hydrologic unit)
A-1	40	4	0.01	Standard Mean
A-2	40	4	0.01	Geometric Mean
A-3	40	4	0	Geometric Mean
B-1	122	11	0.01	Geometric Mean + 1 Standard Deviation
B-2	122	11	0.01	Geometric Mean - 1 Standard Deviation
C-1	122	7	-1.0	Geometric Mean + 1 Standard Deviation
C-2	122	7	0.0125	Geometric Mean - 1 Standard Deviation
C-3	122	7	Pluvial*	Geometric Mean

# Schematic drawing of 4 unit 1-dimensional model



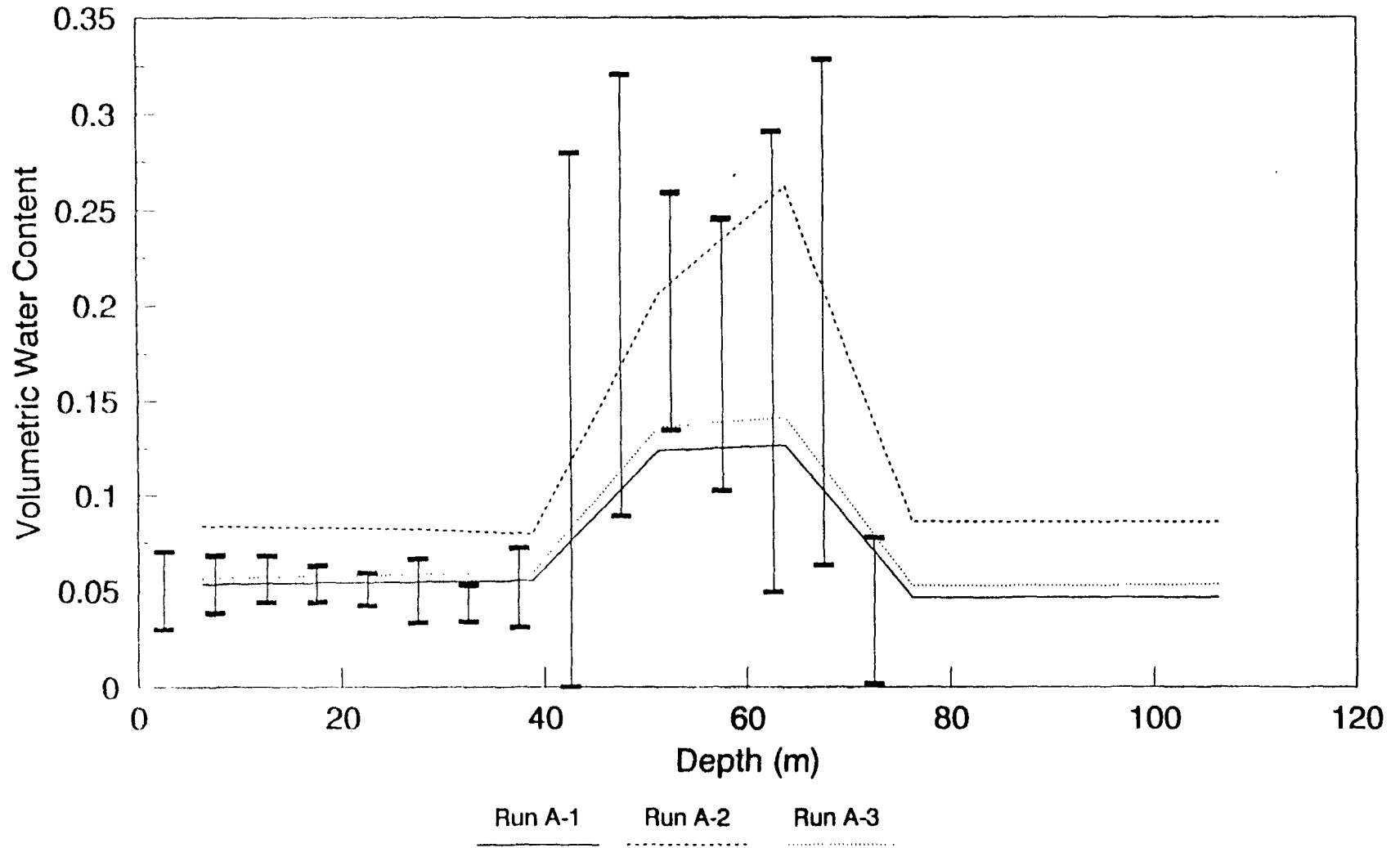
**4 Unit, One-dimensional matrix model properties.**

Unit	Depth Interval (m)	$K_s$ (cm/s)	Porosity
1	0 - 40	5.25E-9	0.093
2	40 - 64	2.64E-6	0.419
3	64 - 396	6.18E-9	0.118
4	396 - 476	4.78E-9	0.240

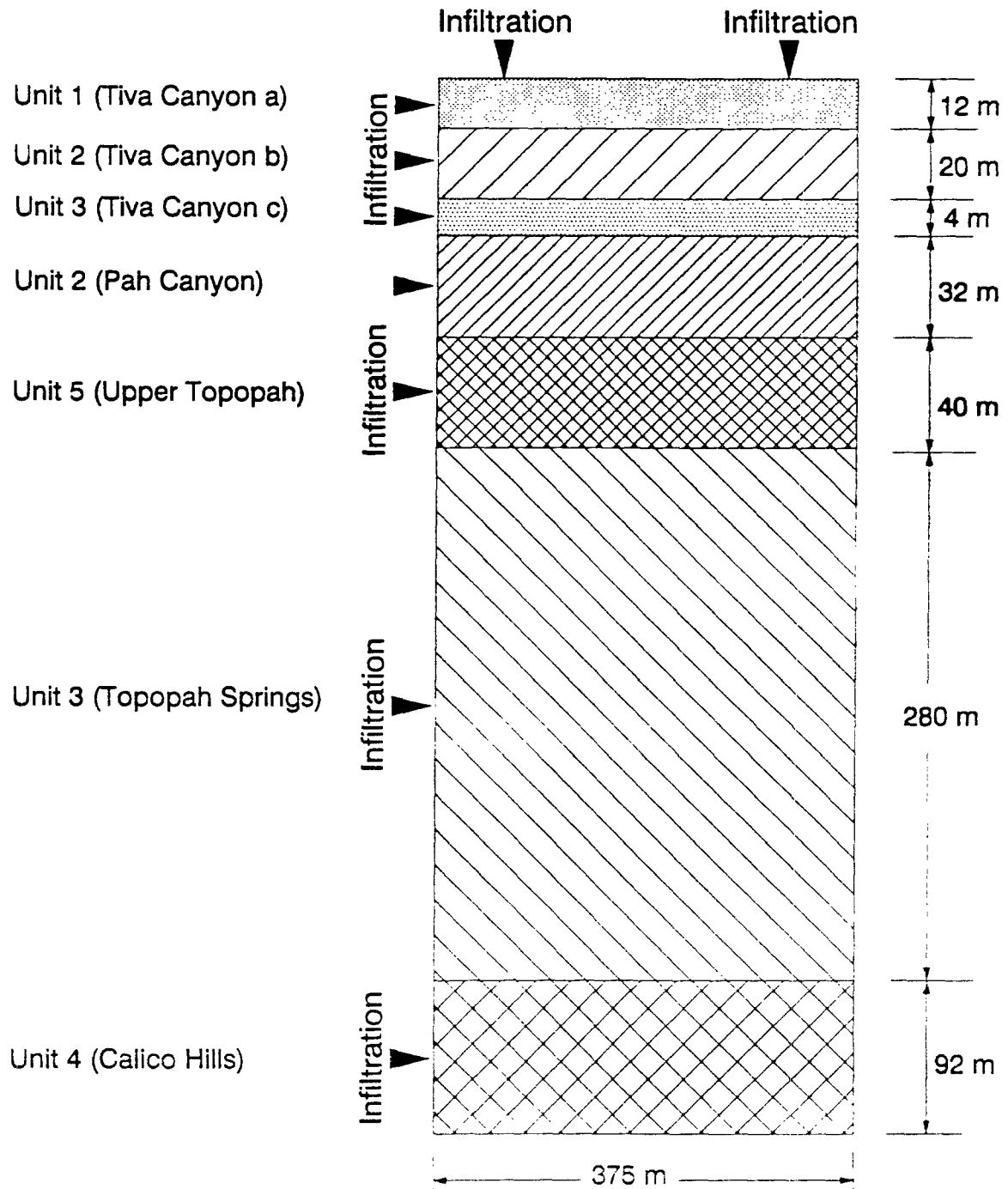
**4 Unit, One-dimensional "Sandia" function properties.**

Unit	Lambda	$S_{ir}$	$S_{is}$	$P_o$	$P_{max}$
1	0.21	0.04	1.0	130,000	5.0E+9
2	0.24	0.04	1.0	22,000	5.0E+9
3	0.24	0.04	1.0	150,000	5.0E+9
4	0.24	0.04	1.0	150,000	5.0E+9

Comparison of Model with 95% Confidence Interval for Measurements



# Schematic drawing of 7 unit 2-dimensional model



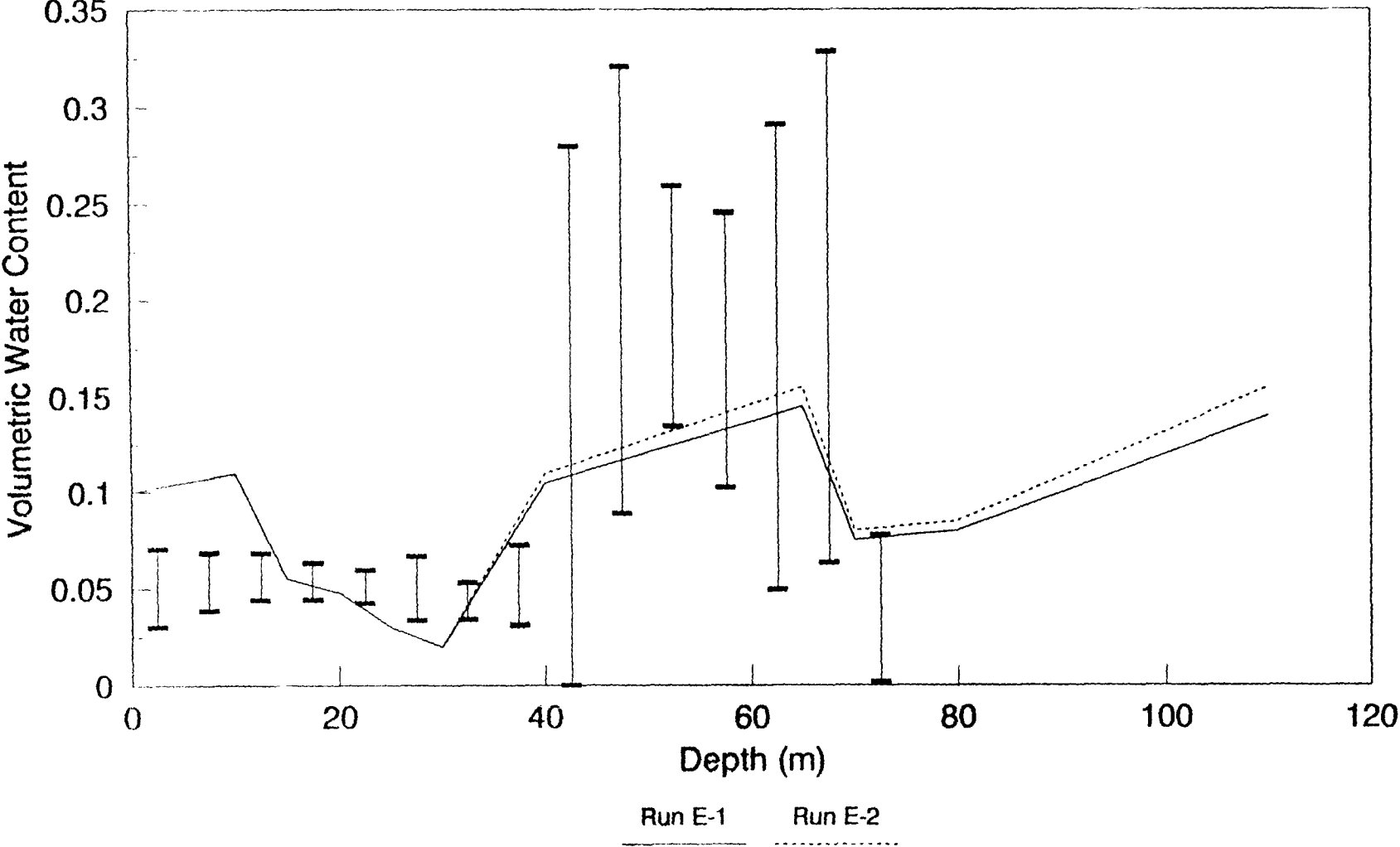
**Hydrologic Properties and Model Geometry for 2-Dimensional Models.**

Geologic Unit	Model Unit	Element #	Thickness (m)	Mean Porosity	Geometric Mean Ksat (cm/s)	StDev Ksat (cm/s)
Tiva Canyon	I	2-4	12	0.140	2.72E-8	2.68E-9
Tiva Canyon	II	5-9	20	0.060	1.35E-9	3.45E-7
Tiva Canyon	III	10	4	0.140	7.79E-8	2.05E-7
Shardy Base, Bedded	IV	11-18	32	0.430	2.68E-4	1.44E-3
Upper Topopah	V	19-28	40	0.160	3.91E-7	1.57E-5
Lower Topopah	VI	29-98	280	0.100	5.14E-10	8.02E-9
Calico Hills	VII	99-121	92	0.240	4.78E-9	7.03E-9

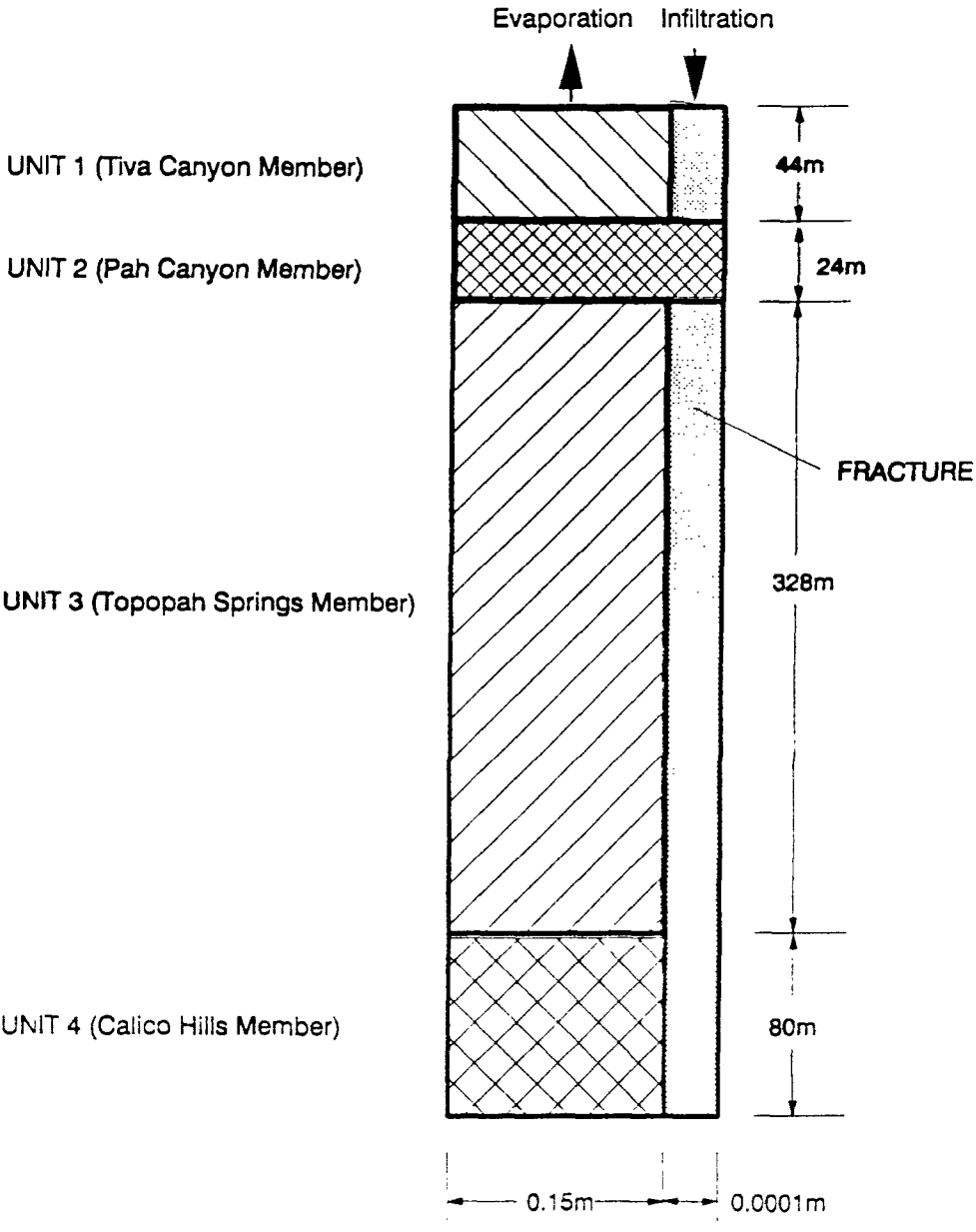
**Sandia Function Parameters for VTOUGH Water Retention Curves for 2-Dimensional Models.**

Unit	Lambda	$S_{lr}$	$S_{ls}$	$1/P_0$ (1/Pa)	$P_{max}$ (Pa)
I	0.33	0.04	1.0	7.41E-6	1.0E+9
II	0.60	0.349	1.0	3.77E-6	1.0E+9
III	0.49	0.01	1.0	4.25E-6	1.0E+9
IV	0.50	0.029	1.0	5.88E-6	1.0E+9
V	0.38	0.04	1.0	9.09E-6	1.0E+9
VI	0.24	0.04	1.0	4.54E-6	1.0E+9
VII	0.20	0.04	1.0	4.17E-6	1.0E+9

Comparison of Model with 95% Confidence Interval for Measurements



# Schematic of conceptual geometry for dual porosity fracture model



**Fracture Model Hydrologic Properties**

UNIT	DEPTH INTERVAL (m)	$K_S$ (m/s)	POROSITY
1	0 - 44	5.25E-11	0.076
2	44 - 68	2.64E-6	0.388
3	68 - 396	6.18E-11	0.118
4	396 - 476	4.78E-11	0.240
FRAC A*	0 - 44 68 - 476	8.15E-3 - 0.130	0.990
FRAC B	0 - 44 68 - 476	8.15E-3 - 0.130	0.990
FRAC C	68 - 476	8.15E-3 - 0.130	0.990

Data from working group composite data and holes UZN-53, UZN-54 and UZN-55.

\* Fracture parameters based on Wang & Narasimhan (1985), and Spengler & Chornack (1984).

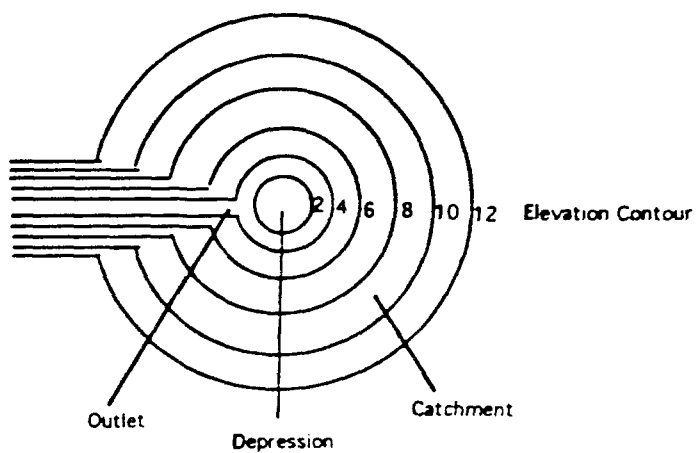
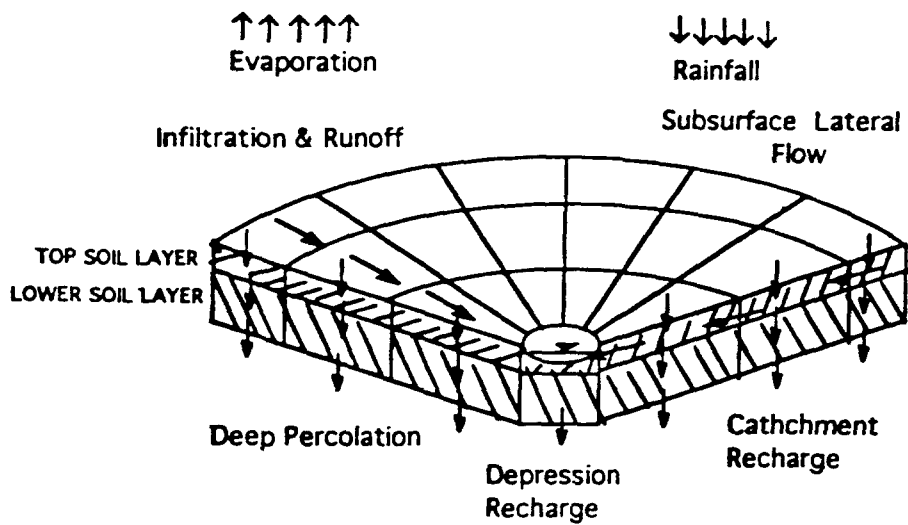
**Fracture Model VTOUGH Sandia Function Parameters**

UNIT	LAMBDA	$S_{lr}$	$S_{ls}$	$1/P_o$ (1/Pa)	$P_{max}$ (Pa)
1	0.21	0.04	1.0	1/130,000	5.0e+9
2	0.24	0.04	1.0	1/22,000	5.0e+9
3	0.24	0.04	1.0	1/150,000	5.0e+9
4	0.24	0.15	1.0	1/150,000	5.0e+9
FRAC A*	0.45	0.04	1.0	1/600	1.0e+9
FRAC B	0.45	0.04	1.0	1/30,000	1.0e+9
FRAC C	0.45	0.04	1.0	1/40,000	1.0e+9

Data from working group composite data and holes UZN-53, UZN-54 and UZN-55.

\* Fracture parameters based on Wang & Narasimhan (1985).

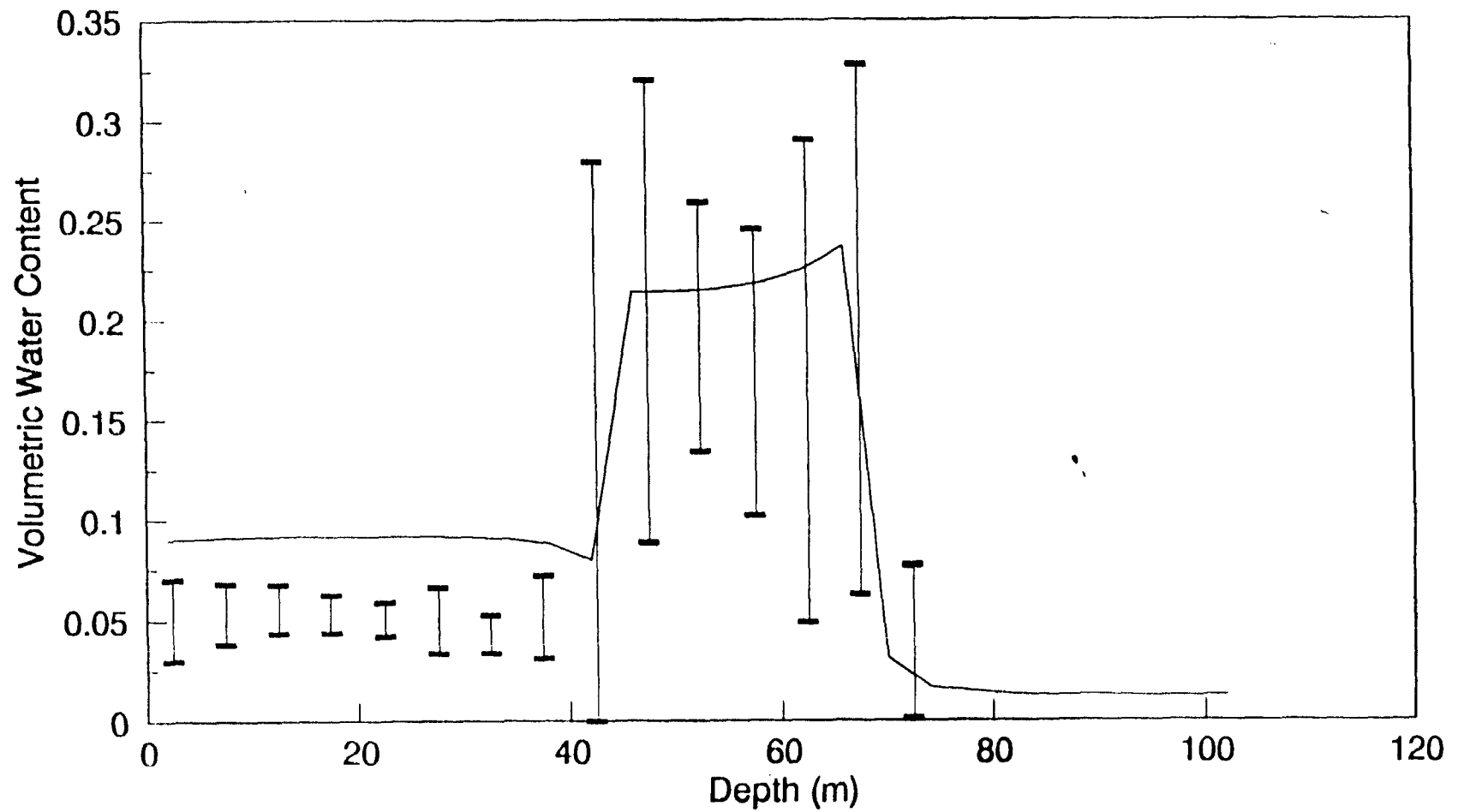
Schematic of conceptual model for Depression Focused Recharge Model  
(Nieber et al., 1993)



**Depression Focus Recharge Model Parameters and Result for Solitario Canyon  
and for Wash Where UZN-53, UZN-54 and UZN-55 are Located.**

Properties	Solitario 1	Solitario 2	Hole Wash 1	Hole Wash 2
Catchment Area (m <sup>2</sup> )	6,157,500	6,157,500	1,242,324	1,242,324
Depression Area (m <sup>2</sup> )	1,131,000	1,131,000	253,388	253,388
Land Slope (deg)	5.7	5.7	5.7	5.7
Albedo	0.3	0.3	0.3	0.3
Outlet Height (m)	0.1	0.1	0.00001	0.01
Catchment Ksat (cm/s)	1.995E-8	1.089E-6	1.99E-7	1.99E-8
Catchment Porosity	0.15	0.15	0.15	0.15
Catchment Soil Storage Parameter (m)	0.099	0.099	0.099	0.099
Catchment Upper Limit of Stage I Evaporation (mm/day <sup>1/2</sup> )	5.2	5.2	5.2	5.2
Depression Ksat (cm/s)	4.0E-4	1.5E-4	4.0E-5	4.0E-4
Depression Porosity	0.51	0.51	0.51	0.51
Depression Soil Storage Parameter (m)	0.099	0.099	0.099	0.099
Depression Upper Limit of Stage I Evaporation (mm/day <sup>1/2</sup> )	5.2	5.2	5.2	5.2
Microdepression Storage (m)	0.0	0.001	0.0	0.001
Depression Recharge (m.yr <sup>-1</sup> )	0.308	0.121	0.008	0.160

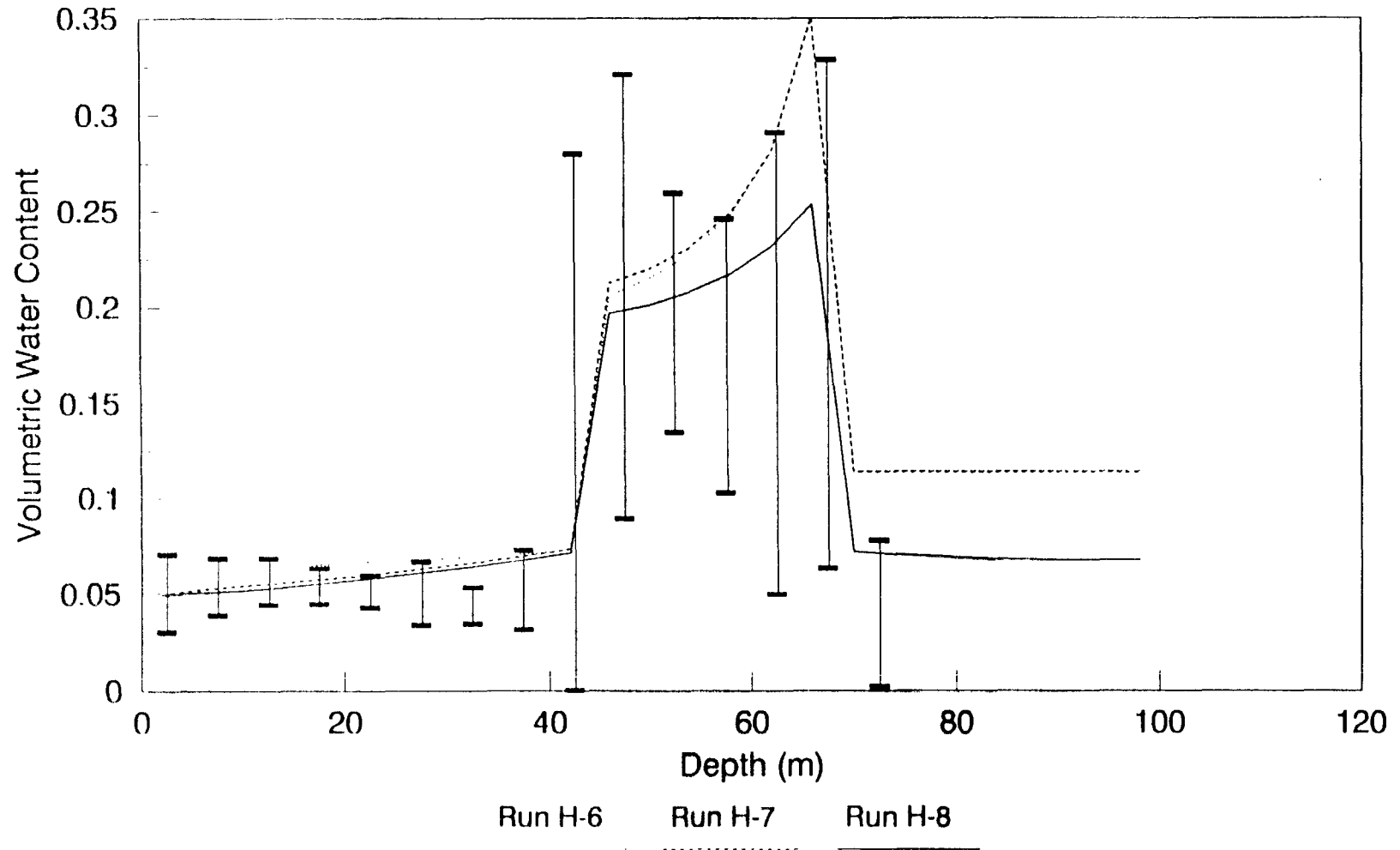
# Single fracture model with 10 cm/yr infiltration for 730 years



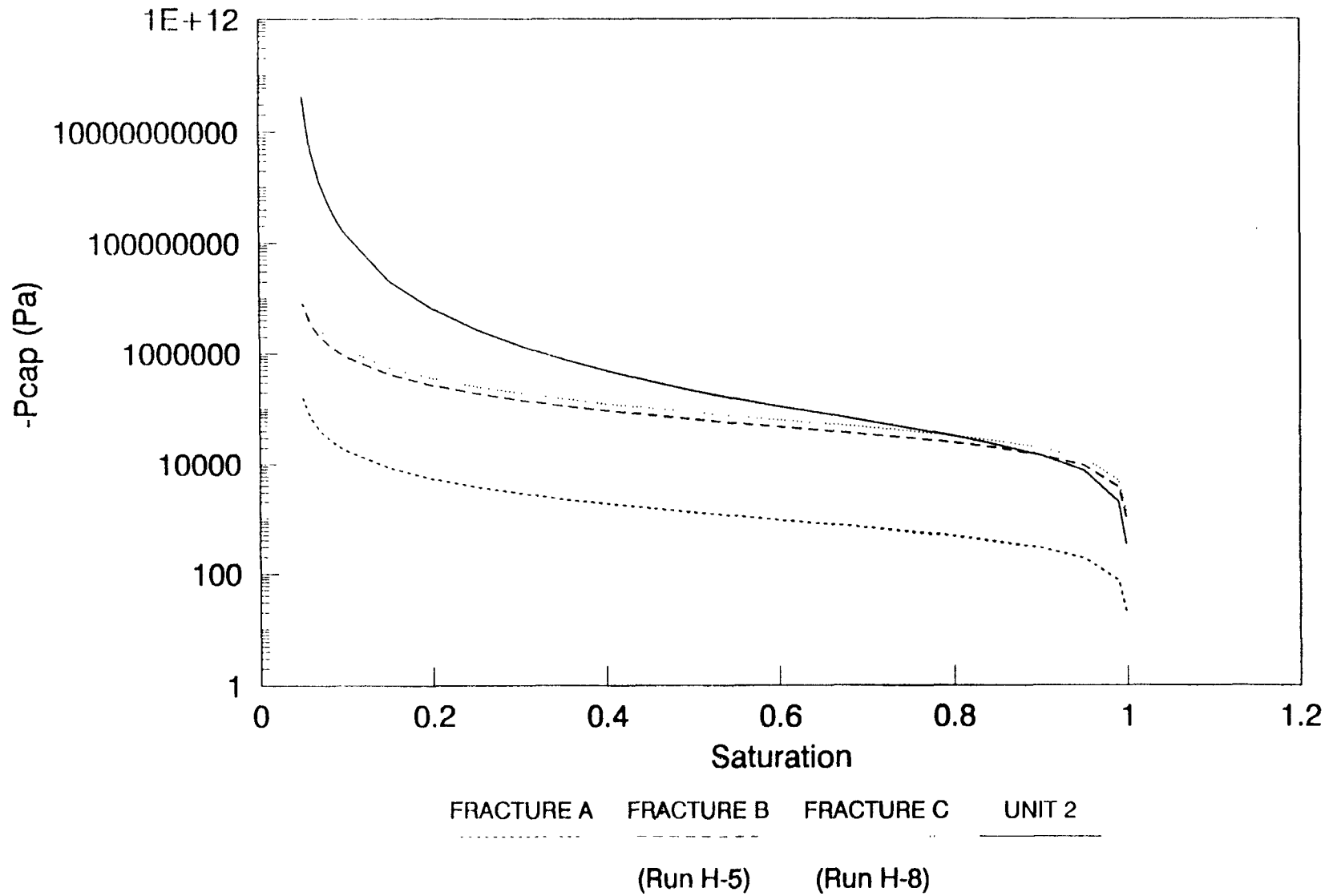
**Fracture Model Features for H Series Runs.**

Run #	Infiltration History	Final Evaporation (mm/yr)	Fracture to Matrix Contact Area	Aperture for Conductivity ( $\mu\text{m}$ )	Fracture Water Retention Curve*
H-1	Pluvial	0.03	1/10	100	A
H-2	2 mm/yr	0.04	1/10	100	A
H-3	0.5 mm/yr	0.02	1/10	100	A
H-4	Pluvial	0.005	1/100	100	A
H-5	Pluvial	0.02	1/10	100	B
H-6	5 mm/yr	0.03	1/10	200	A
H-7	10 mm/yr	0.008	1/10	400	A
H-8	5 mm/yr	0.009	1/10	400 (upper) 300 (lower)	A (upper) C (lower)

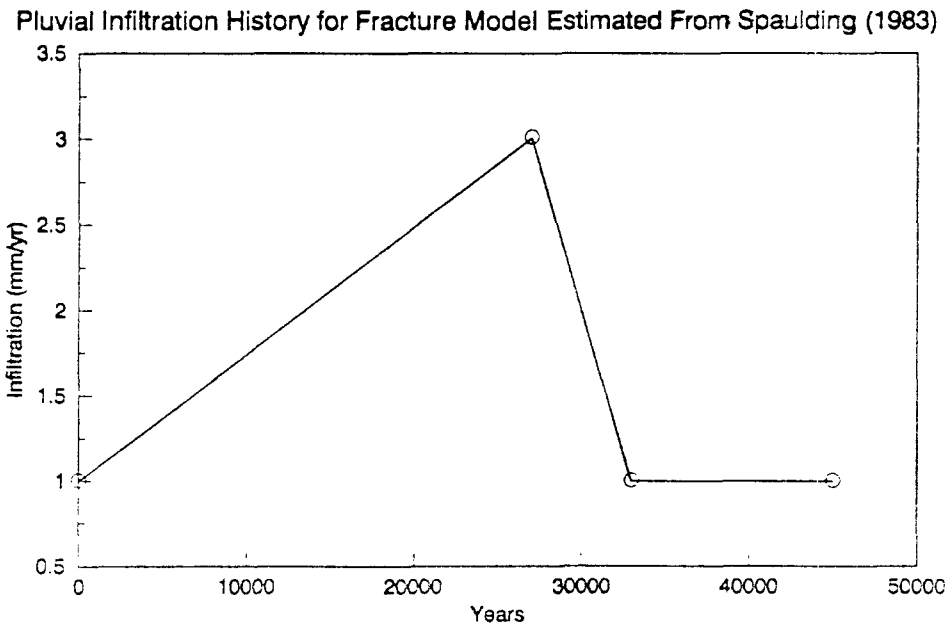
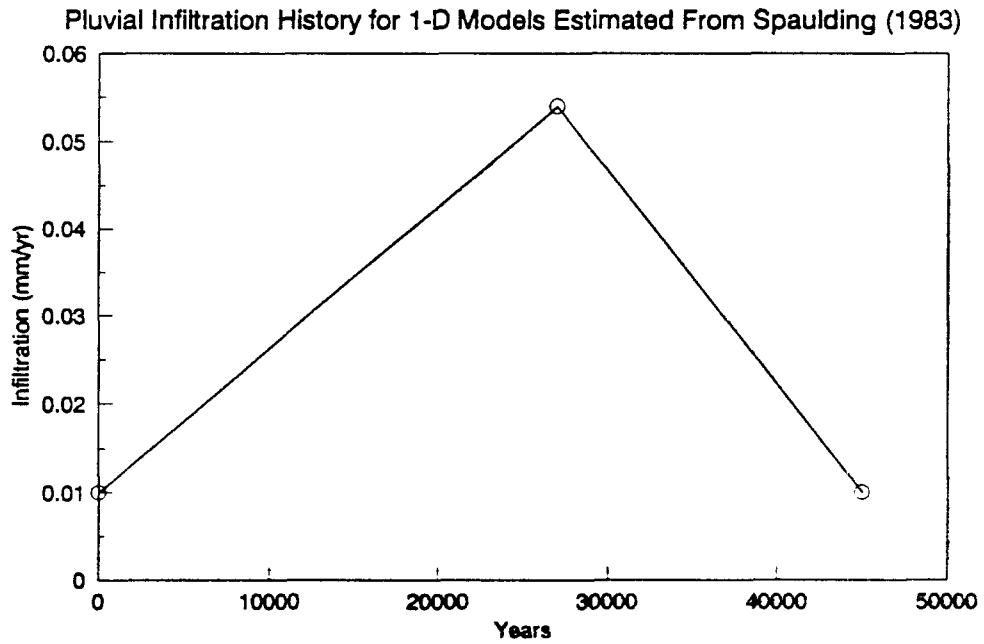
Comparison of Model with 95% Confidence Interval for Measurements



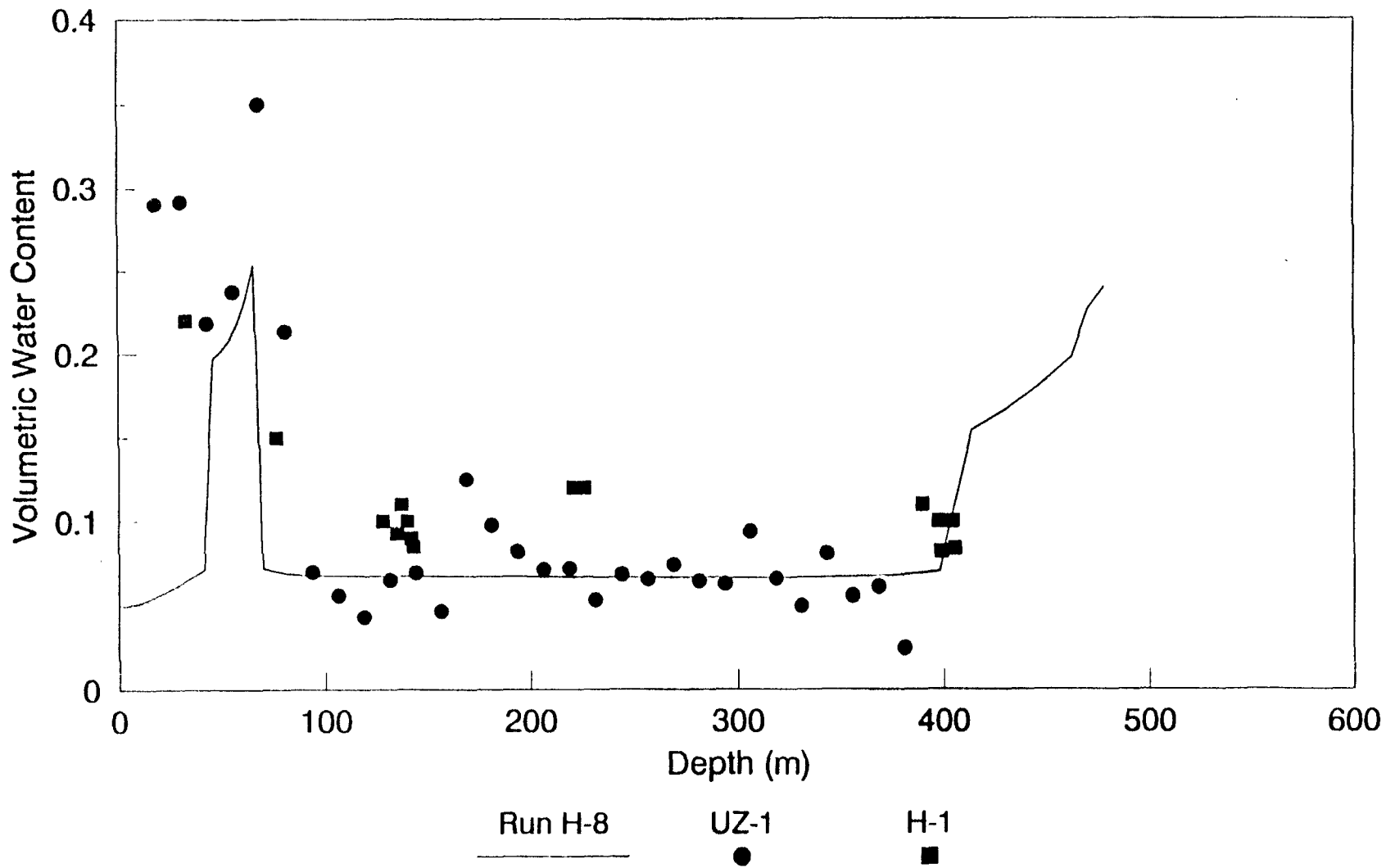
Modeled Water Retention Curves for Fractures A, B and C compared to Unit 2



Infiltration signals based on both of Spaulding's (1983) interpretations of his rat midden data.



Comparison of Model Run H-8 with Measured Volumetric Water Contents



## CONCLUSIONS

1. NON-UNIQUE SOLUTION
  
2. OTHER CONFIRMATORY PARAMETERS NEEDED
  - AT MINIMUM A CONFIRMATORY PARAMETER TO FIX TIME HISTORY OF FLUID -  $^{14}\text{C}$  - TRITIUM OR OTHER ISOTOPES
  
  - TIME SERIES OF TEMPERATURE IN UNSATURATED ZONE (SASS, 1988)
  
3. DATA NEEDS
  - FRACTURE INFORMATION - APERTURE, CONDUCTIVITY, AND CHARACTERISTIC CURVES
  
  - DATA FROM FOCUSING AREAS
  
4. OTHER POTENTIALLY USEFUL INFORMATION
  - CONFIRMATORY
  
  - CONSISTENCY

## **POTENTIALLY USEFUL DATA - SATURATED ZONE**

- **WATER TABLE ELEVATIONS**
- **WATER TABLE FREQUENCIES**
- **WATER TABLE TEMPERATURE DISTRIBUTIONS**

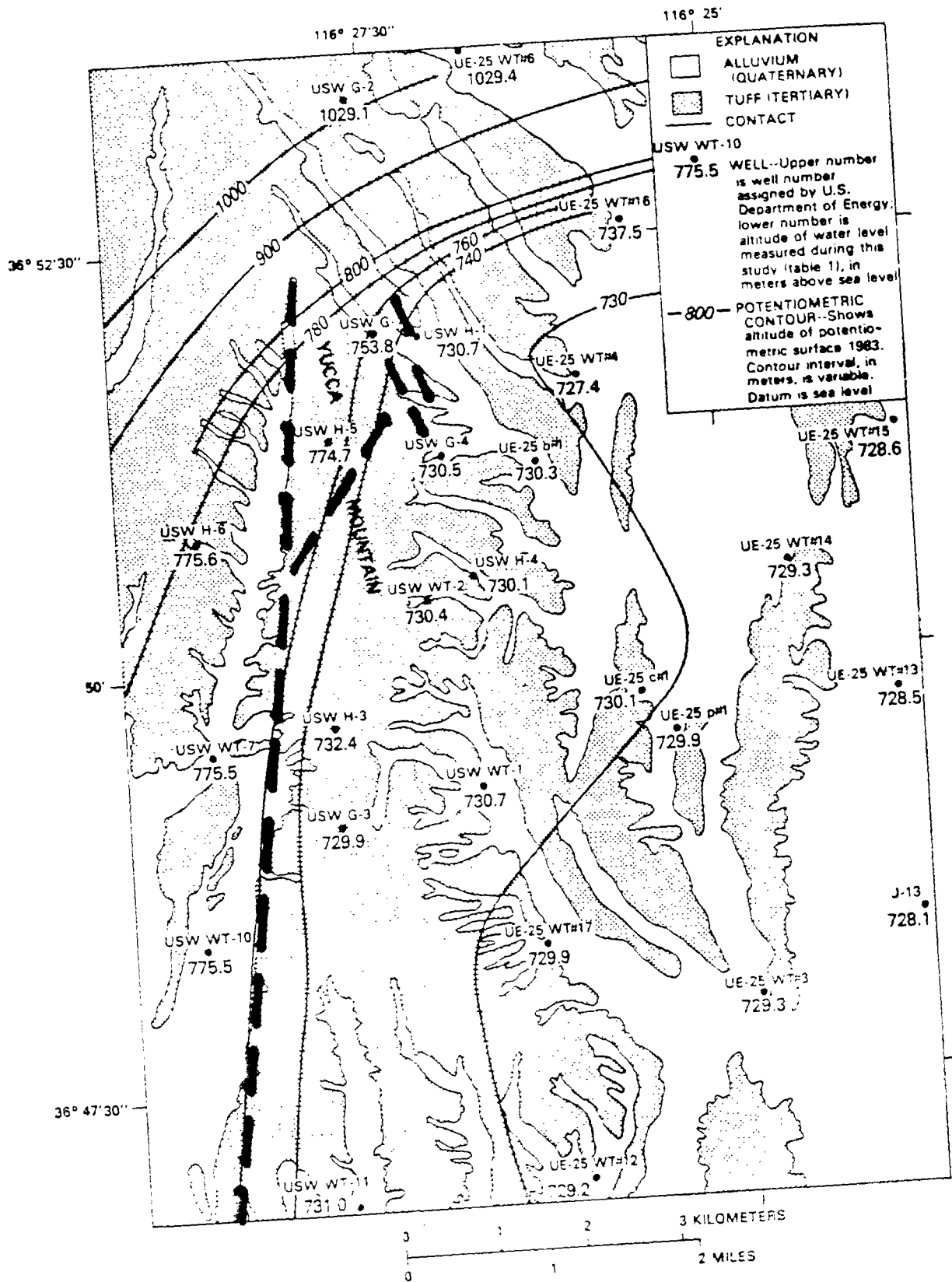
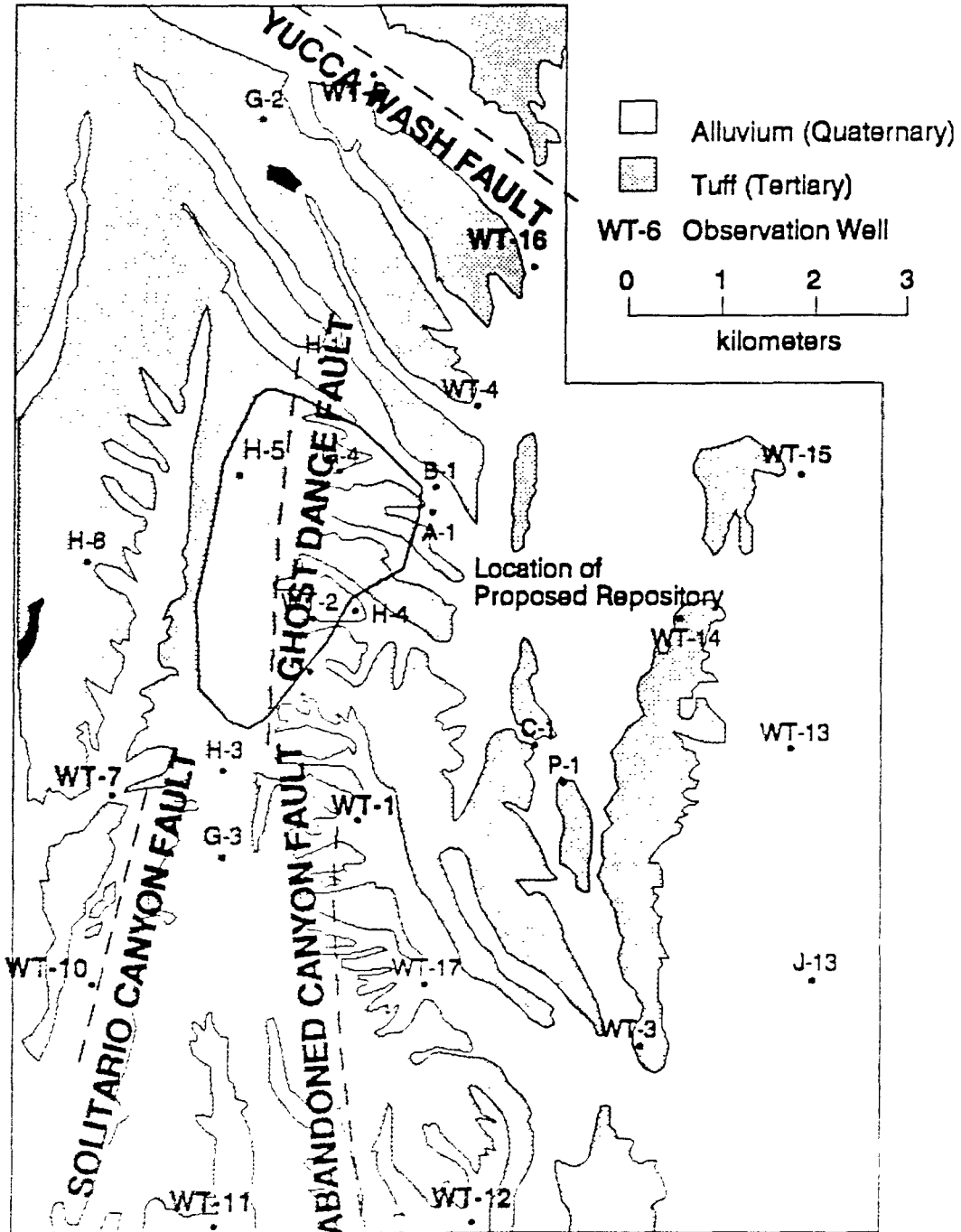


Figure 2.--Preliminary potentiometric-surface map, Yucca Mountain.

# Location of Faults at Yucca Mountain

## Selected Faults in Study Area

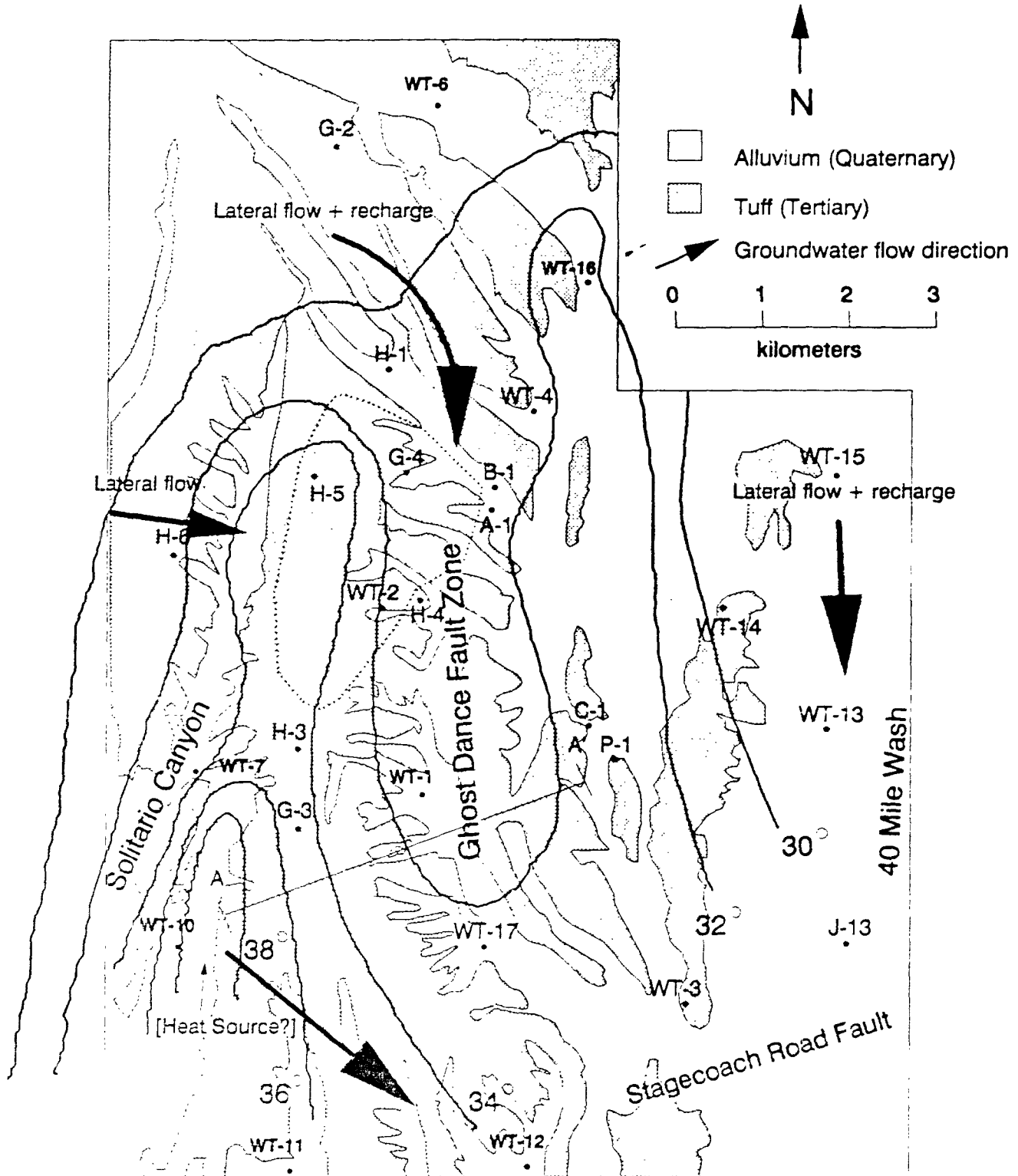


L. Lehman & Associates, Inc.

1990



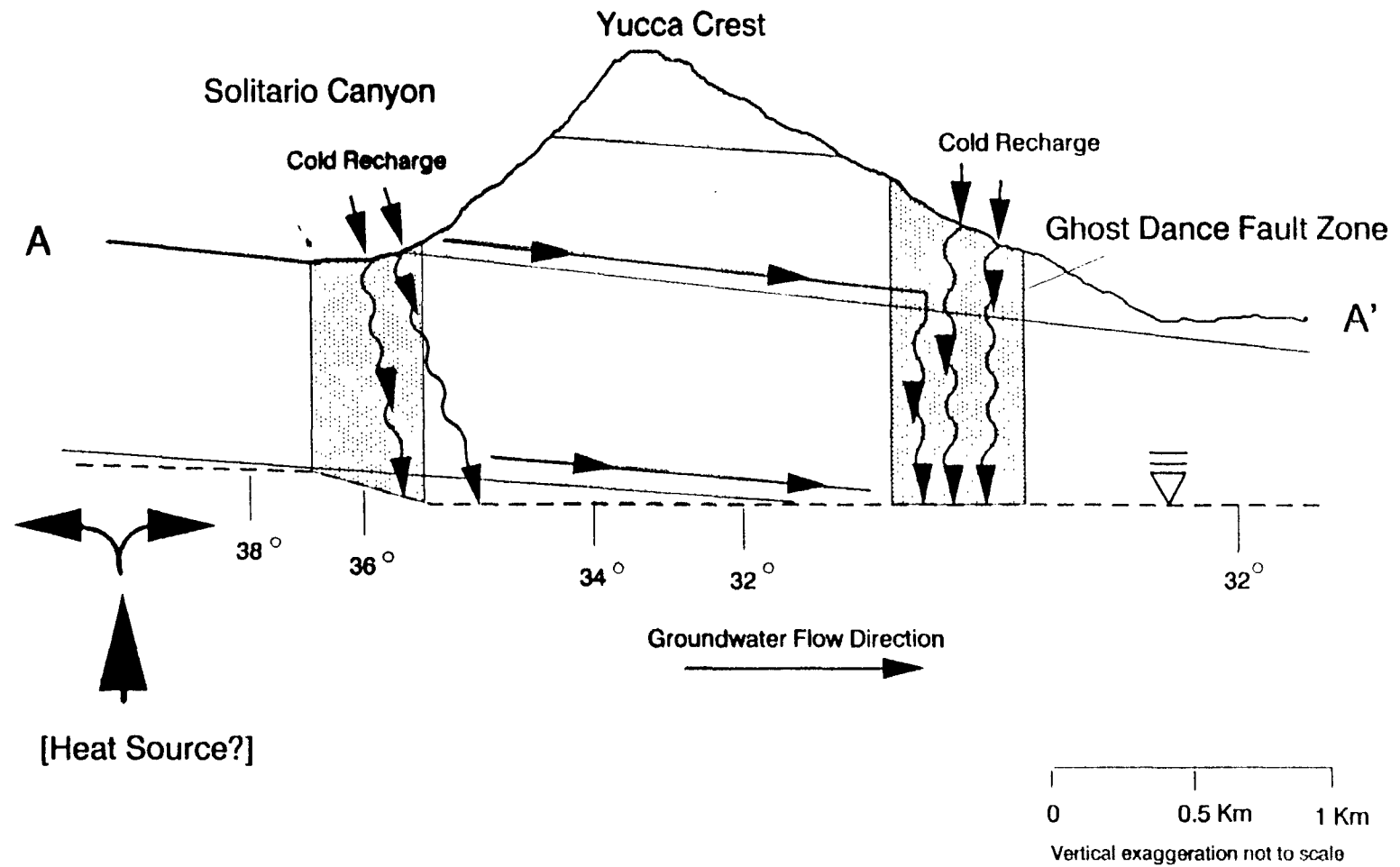
# Saturated Zone - Water Table Isotherms



L. Lehman & Associates, Inc.

1993

# Infiltration Conceptual Model Compared to Isotherms



L. Lehman & Associates, 1993

Well #	Period	Phase Shift	Amplitude	r <sup>2</sup>	Slope	Cycles
WT-7	1012.2	177.7	0.09	0.47	0.000107	1½ cycle
WT-10	925.4	182.4	0.7	0.22	0.000074	~ 2 cycles
WT-12	1240.0	169.8	0.7	0.35	0.000101	~ 1½ cycles
WT-1	889.2	249.5	0.1	0.44	.000191	almost 2 cycles
WT-11	887.7	253.4	0.115	0.58	0.000100	~ 1½ cycles
WT-16	860.6	266.9	0.11	0.68	0.000240	~ 1½ cycles
WT-6	2975.2	738.1	1.3	0.75	.00323	~ ½ cycle
H-5	1936.8	416.6	0.54	0.45	-0.000044	< ½ cycle
H-5	1888.4	417.9	0.31	0.28	-0.00033	~ ½ cycle
WT-1*	1597.8	159.5	0.0625	0.32	-0.000085	~ 1 cycle
WT-10*	935.5	163.3	0.0565	0.22	0.000083	~ 1½ cycles
WT-16* Fit 1	226.4	279.7	-0.0365	0.24	-0.000130	~ 5½ cycles
WT-16* Fit 2	1229.4	143.2	0.0385	0.22	-0.000130	½ cycle

\*Indicates offsets were subtracted from original data.

**DRAFT**

**DRAFT**

Testing Conceptual Unsaturated Zone Flow Models Using Numerical Simulation of Real Data for the Proposed High Level Nuclear Waste Repository at Yucca Mountain, Nye County, Nevada

Tim P. Brown  
Linda L. Lehman  
John L. Nieber

T.P. Brown and L.L. Lehman (L. Lehman & Associates, Inc. 1103 W. Burnsville Pkwy, Suite 209, Burnsville MN 55337; 612-894-0357

J.L. Nieber (Agricultural Engineering, University of Minnesota, 1390 Eckles Ave. St. Paul MN 55108; 612-625-6724

**Abstract**

An important component of site characterization and suitability assessment of the proposed nuclear waste repository at Yucca Mountain, Nevada is determination of the best conceptual model of the hydrologic mechanisms governing saturated and unsaturated flow on and around the site. As observers in the INTRAVAL Unsaturated Zone Working Group, L. Lehman & Associates developed several modeling studies of the unsaturated zone at Yucca Mountain. Information was provided to the Working Group by the USGS. Additional published data were utilized to fill in data gaps and to provide additional confidence in results.

Data were modeled utilizing one and two dimensional matrix and fracture numerical models. Runoff and infiltration models were also utilized to verify boundary conditions. The geologic processes and characteristics modeled include, zonation of hydrologic properties, matrix flow, fracture flow, fracture/matrix interaction, evaporation and transpiration, focused infiltration and transient infiltration.

Infiltration estimates for the site based on our modeling and estimates by others, have consistently been much higher than the maximum capable by matrix flow alone. Consideration of fracture flow, as in our modeling, allows the higher infiltration rates and retains agreement between actual and modeled water content data.

One and two dimensional simulations of unsaturated matrix flow did a poor job of matching the data. We have obtained good agreement using a 2-dimensional dual porosity fracture flow model. We conclude an additional measure is needed to constrain the field conditions enough to validate conceptual models using numerical models. Specifically, geochemical analysis such as tritium, chlorine-36 or carbon-14, which can give estimates of time since recharge for water in the unsaturated zone, are needed to eliminate the non-uniqueness of various model solutions.

## 1. Introduction

As an observer in the International Transport Code Validation Study (INTRAVAL) Unsaturated Zone Working Group, L. Lehman & Associates developed and examined results of several modeling studies of the unsaturated zone at Yucca Mountain, Nye County, Nevada. Information was provided to the Working Group by the USGS for three shallow boreholes, UZN-53, UZN-54, and UZN-55. Additional published data were utilized as well to help fill in data gaps and to provide additional confidence in results. The INTRAVAL working group modelers were to model the unsaturated flow through Yucca Mountain using any data available to them and using their own preferred modeling techniques. Their modeled water contents along a vertical profile would ultimately be compared to water content data from a deep hole (UZN-16) currently being drilled near the above mentioned shallow holes. The goal of the study was to validate the best model of unsaturated flow through Yucca Mountain based on the models' ability to predict water content conditions at UZN-16.

The numerical simulators chosen by L. Lehman & Associates to model the unsaturated flow were the VTOUGH code developed at Lawrence Berkeley Laboratory (Pruess, 1987), and the TWOD code of Nieber et al. (In press). We modeled the data set utilizing 1-dimensional matrix, 2-dimensional matrix and dual porosity fracture conceptual models. We also utilized models which calculated runoff and infiltration in order to verify boundary conditions.

Our initial conceptual model of unsaturated flow at Yucca Mountain was that of uniform infiltration along the upper surface of the volcanic tuff stratigraphy. Flow was assumed to occur predominately through the matrix from the surface, through the repository horizon at the Topopah Springs Member, continuing to the water table. This conceptual model evolved, based on model simulations, to include fracture flow and focused recharge mechanisms. The ultimate geologic processes and characteristics seen as important to the unsaturated flow regime as analyzed by Lehman (1992), Montazer and Wilson (1984), and others, were included in the modeling. These processes and characteristics include:

- zonation of hydrologic properties
- matrix flow
- fracture flow
- fracture/matrix interaction
- evaporation and transpiration
- focused infiltration
- transient infiltration.

Table 1 details the processes included in each model along with justification and data sources for each of them.

Table 1: Important Modeled Processes in L. Lehman & Associates Yucca Mountain Unsaturated Zone Models.

PROCESS	MODELS	BASIS	DATA SOURCES
Zonation of hydrologic properties	1-D 2-D DFR FRACTURE	Geologic coring and mapping	<ul style="list-style-type: none"> <li>• Working group data (USGS)</li> <li>• Hole data from UZN holes 53, 54 and 55</li> </ul>
Matrix flow	1-D 2-D DFR FRACTURE	Predominance of wet porous media	<ul style="list-style-type: none"> <li>• Working group data (USGS)</li> <li>• Hole data from UZN holes 53, 54 and 55</li> <li>• Tyler, (1987)</li> </ul>
Fracture flow	FRACTURE	<ul style="list-style-type: none"> <li>• High fracture densities</li> <li>• Wet fractures observed in drilling UZN-54 &amp; 55</li> <li>• Lehman (1992)</li> <li>• Montazer &amp; Wilson (1984)</li> </ul>	<ul style="list-style-type: none"> <li>• Spengler &amp; Chornack (1984)</li> <li>• Wang &amp; Narasimhan (1985)</li> </ul>
Fracture/matrix interaction	FRACTURE	<ul style="list-style-type: none"> <li>• Existence of fracture coatings</li> <li>• Existence of transient infiltration</li> </ul>	Thoma et al. (1992)
Evaporation	DFR FRACTURE	<ul style="list-style-type: none"> <li>• High solar radiation in desert terrain</li> <li>• DFR model of Nieber et al. (1993)</li> </ul>	U.S. Weather Service
Focused infiltration	2-D DFR FRACTURE	<ul style="list-style-type: none"> <li>• Topography</li> <li>• Large conductivity contrasts in materials</li> </ul>	<ul style="list-style-type: none"> <li>• Nieber et al. (1993)</li> <li>• Harrill et al. (1988)</li> <li>• Hokett et al. (1991)</li> </ul>
Transient infiltration	1-D 2-D DFR FRACTURE	Long time frame with high probability of climate change	Spaulding (1983)

We conclude that neither the 1-dimensional nor 2-dimensional models did as good a job of matching the water content data as did the subsequent fracture model. Further, the problem is not well posed as a validation exercise because the solutions are non-unique. More constraints are needed either to boundary or initial conditions to further analyze or compare results. Additionally, we conclude that more than one performance measure must be utilized to determine if any given model is a valid representation. For example, comparison to tritium data could be extremely useful in this INTRAVAL problem to constrain the time since infiltration of surface water.

## 2. 1-Dimensional Model

For the 1-dimensional, and later dual porosity fracture models, an integrated finite difference computer code V-TOUGH (Nitao, 1990), which is an enhanced version of the TOUGH code (Pruess, 1987), was used. This simulator calculates multi-phase fluid flow in unsaturated porous media under non-isothermal conditions. For this study isothermal conditions were assumed and enforced upon the model simulations.

The 1-dimensional VTOUGH simulations consist of 4, 7 and 11 hydrologic unit configurations representing the stratigraphic column at Yucca Mountain. They are based on the composite data provided by the USGS and use 3 different infiltration scenarios. The properties and geometry of the 7 unit model are given in Table 2. Hydrologic units were inferred from the composite data provided by the USGS, based on qualitative grouping of similar valued measured properties. Conductivities were estimated as the geometric mean of measured conductivities from inferred units. Porosity and other properties are taken as the standard mean. Parameters used in the VTOUGH Sandia Function (modified van Genuchten Equation) to represent the water retention characteristics were fitted to the available water retention data by minimizing the sum of the squared error between the function and the data. Water retention parameters used for this model are presented in Table 3.

### Boundary Conditions

The upper boundary of the matrix and fracture elements simulate atmospheric conditions. Gas pressure at the upper boundary was fixed at 100,000 Pa (1 atm) and saturation near 0 for the simulations. The lower boundary of matrix and fracture elements simulate conditions at the water table. Pressure here was fixed at 100,000 Pa and saturation at 1. The left and right domain boundaries are modeled as no flow boundaries.

### Initial Conditions And Infiltration History

The initial state of the model elements is such that the column is nearly in equilibrium with about 0.005 mm/yr of downward flow. Two steady state infiltration rates, 0 and 0.01 mm/yr, were used along with a transient "pluvial" infiltration signal. The pluvial infiltration history is based on work done by Spaulding (1983). It is modeled starting

Table 2. Hydrologic Properties and Model Geometry for 1-Dimensional C series and 2-Dimensional Models.

Geologic Unit	Model Unit	Element #	Thickness (m)	Mean Porosity	Geometric Mean Ksat (cm/s)	StDev Ksat (cm/s)
Tiva Canyon	I	2-4	12	0.140	2.72E-8	2.68E-9
Tiva Canyon	II	5-9	20	0.060	1.35E-9	3.45E-7
Tiva Canyon	III	10	4	0.140	7.79E-8	2.05E-7
Shardy Base, Bedded	IV	11-18	32	0.430	2.68E-4	1.44E-3
Upper Topopah	V	19-28	40	0.160	3.91E-7	1.57E-5
Lower Topopah	VI	29-98	280	0.100	5.14E-10	8.02E-9
Calico Hills	VII	99-121	92	0.240	4.78E-9	7.03E-9

Table 3. Sandia Function Parameters for VTOUGH Water Retention Curves for 1-Dimensional C Series and 2-Dimensional Models.

Unit	Lambda	S <sub>lr</sub>	S <sub>ls</sub>	1/P <sub>0</sub> (1/Pa)	P <sub>max</sub> (Pa)
I	0.33	0.04	1.0	7.41E-6	1.0E+9
II	0.60	0.349	1.0	3.77E-6	1.0E+9
III	0.49	0.01	1.0	4.25E-6	1.0E+9
IV	0.50	0.029	1.0	5.88E-6	1.0E+9
V	0.38	0.04	1.0	9.09E-6	1.0E+9
VI	0.24	0.04	1.0	4.54E-6	1.0E+9
VII	0.20	0.04	1.0	4.17E-6	1.0E+9

Table 4. 1-Dimensional Simulation Features.

Simulation Designator	# of Model Elements	# of Hydrologic Units	Infiltration Model (mm/yr)	Saturated Conductivity Model (per hydrologic unit)
A-1	40	4	0.01	Standard Mean
A-2	40	4	0.01	Geometric Mean
A-3	40	4	0	Geometric Mean
B-1	122	11	0.01	Geometric Mean + 1 Standard Deviation
B-2	122	11	0.01	Geometric Mean - 1 Standard Deviation
C-1	122	7	-1.0	Geometric Mean + 1 Standard Deviation
C-2	122	7	0.0125	Geometric Mean - 1 Standard Deviation
C-3	122	7	Pluvial*	Geometric Mean

\* See Figure 3 for details.

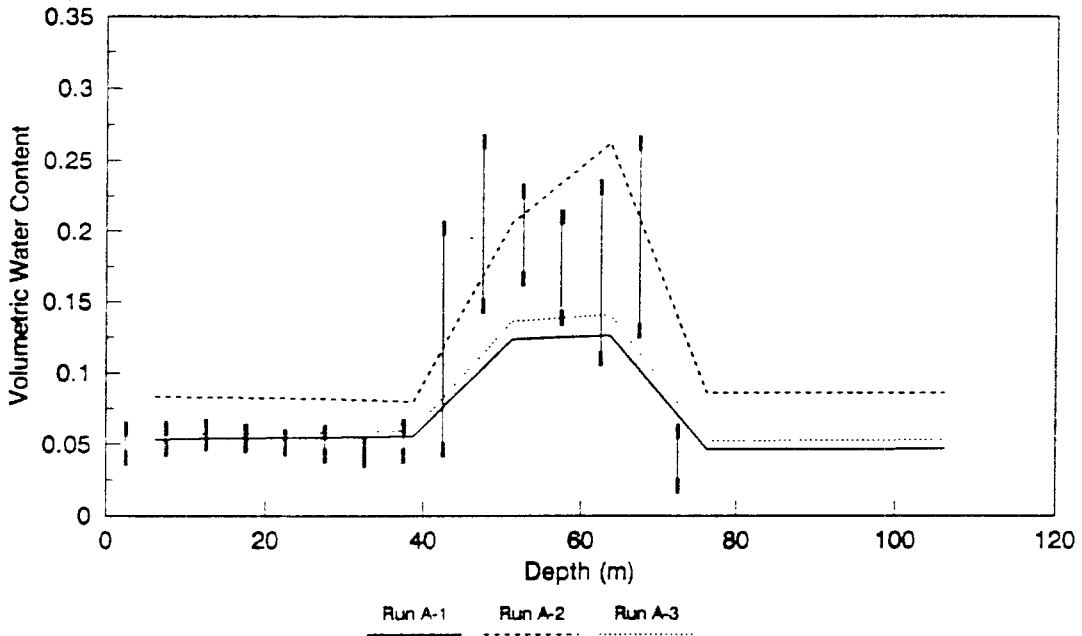
45,000 years ago with 0.01 mm/yr infiltration which increases linearly to a pluvial maximum at about 18,000 years ago with infiltration of 0.054 mm/yr and then decreases linearly back to 0.01 mm/yr at the present. The infiltration was applied at the uppermost model element as a water source.

### Summary of Results

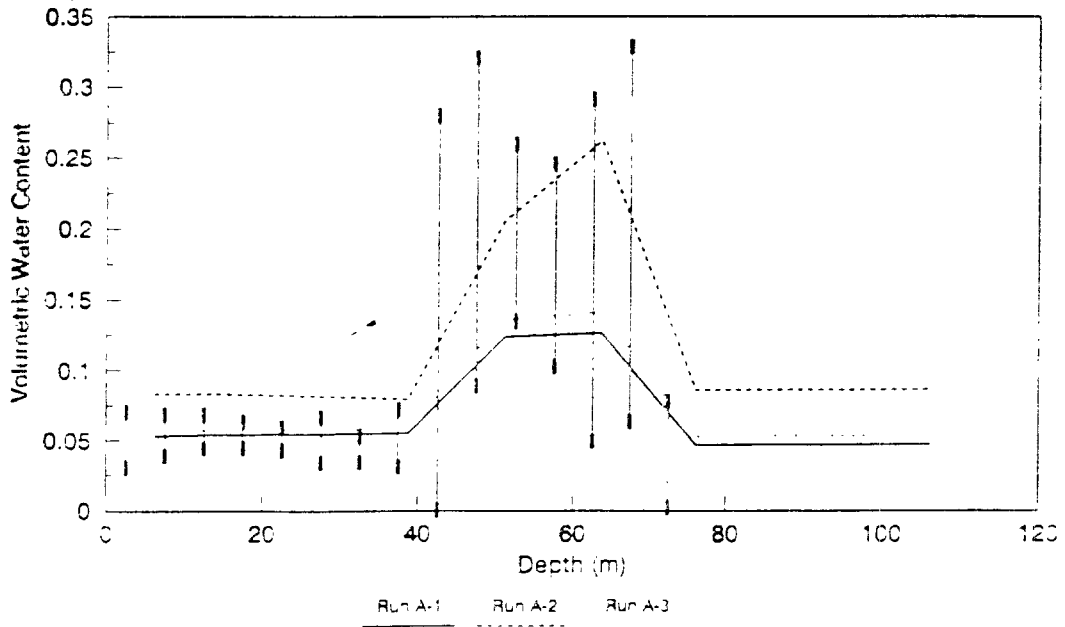
The results of the 4 unit, 1-dimensional simulations are shown in Figure 1. The modeled water content profile is plotted versus depth and compared to hole data 95% confidence intervals and 68% confidence intervals. The measured water content confidence intervals are found by grouping the data to include all measurements found in each 5 meter span. Statistics were then calculated for each 5 meter "sample" and intervals were calculated as 2 standard deviations below the mean to 2 standard deviations above the mean for the 95% interval and as 1 standard deviation below the mean to 1 standard deviation above the mean for the 68% interval. Depth measurements were slightly adjusted to align obvious stratigraphic contacts based on porosity measurements in the data. The number of data points in each 5 meter group ranged from 13-21 and averaged 18.3. The water content profiles are emphasized

Figure 1. Comparison of simulated water contents using the 1-dimensional 4 unit runs with confidence intervals for working group data from shallow holes UZN-53, UZN-54 and UZN-55.

Comparison of Model with 68% Confidence Interval for Measurements



Comparison of Model with 95% Confidence Interval for Measurements



because this quantity is actually measured at the boreholes and this was chosen as the calibration measure by the INTRAVAL working group. Simulated water content profiles are shown nearly at steady state except for the runs using the pluvial infiltration signal which covers 45,000 years then terminates.

Simulations A-1 and A-2 compare the effect of choosing the standard mean or the geometric mean of saturated hydraulic conductivity data for the model hydrologic unit values. The standard mean of A-1 gives conductivity values weighted toward the high end and results in lower water content within the units at equilibrium. The geometric mean gives a lower value more central to the near lognormal distribution of conductivity data resulting in a wetter equilibrium water content profile. Both of these simulations used an infiltration rate of 0.01 mm/yr which is near the maximum that the geometric mean of the upper unit conductivity will allow without ponding. Using the geometric mean model for conductivity values, but reducing infiltration input to zero in run A-3 nearly duplicates run A-1. Even after nearly 10,000,000 years of simulation time, flow within Run A-3 does not go entirely to 0 but has diminished to about 0.0002 mm/yr along the column. This explains the slightly higher water contents found in Run A-3 over Run A-1, which has higher infiltration input along with higher conductivity. It is apparent here that many combinations of conductivity values and infiltration rates may be used to calculate virtually the same water content profile.

Overall this model configuration does not do a good job of predicting the measured data. Runs A-1 and A-3 match the data fairly well to a depth of 40 meters but appear too dry from 40 to 70 meters. While run A-2 matches the data better at 40 to 70 meters it is too wet from 0 to 40 meters. The lower water content areas of the profile appear high, relative to the high water content zone at 40 to 70 meters, or conversely, the 40 to 70 meter zone is modeled relatively dry compared to adjacent zones.

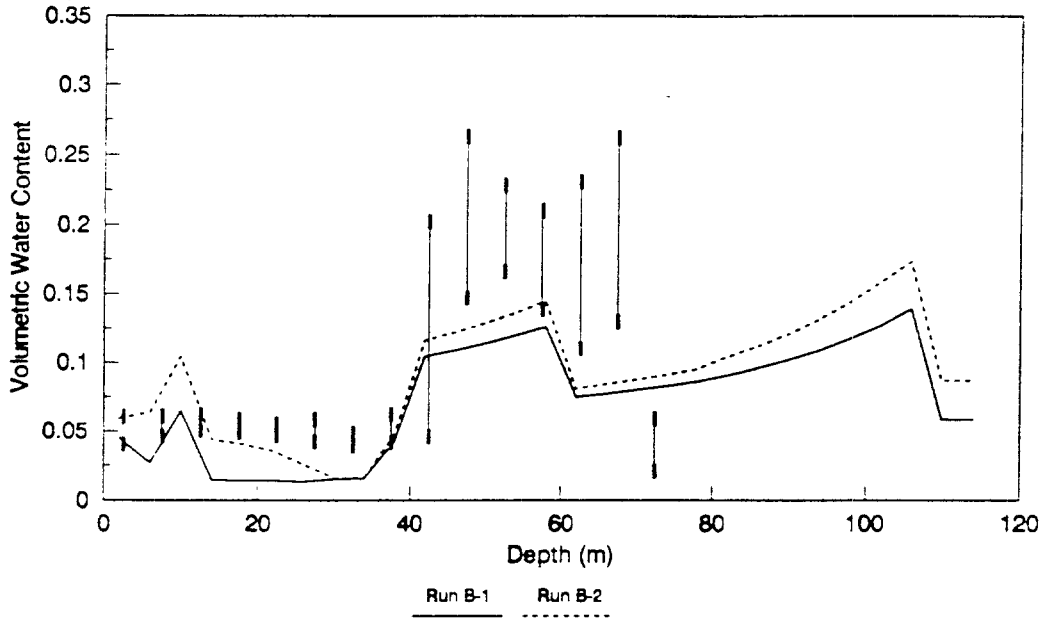
Figure 2 presents the results of the 11 unit, 1-dimensional model simulations. Run B-1 uses hydraulic conductivities 1 standard deviation above the geometric mean while run B-2 uses conductivities 1 standard deviation below the geometric mean. The infiltration rate was set to 0.01 mm/yr, near the rate at which saturation occurs in the least conductive units, a condition not known to exist at the time of this study.

The variation in modeled water content observed here due to an order of magnitude, or so, adjustment in hydraulic conductivity is surprisingly small. This would seem to suggest that the model is not terribly sensitive to conductivity error of this degree. It is also observed that the modeled profile tends to be lower than the data even at this upper limit of reasonable matrix infiltration given the measurements. The shape of the curve also poorly coincides with that measured. The modeled profile appears to be more complex than the data possibly indicating that too many units were derived from the original hydrologic measurements.

Results from the 7 unit, 1-dimensional model simulations are presented in Figure 4. These simulations used three hydraulic conductivity models. Run C-1 used the

Figure 2. Comparison of simulated water contents using the 1-dimensional 11 unit runs with confidence intervals for working group data from shallow holes UZN-53, UZN-54 and UZN-55.

Comparison of Model with 68% Confidence Interval for Measurements



Comparison of Model with 95% Confidence Interval for Measurements

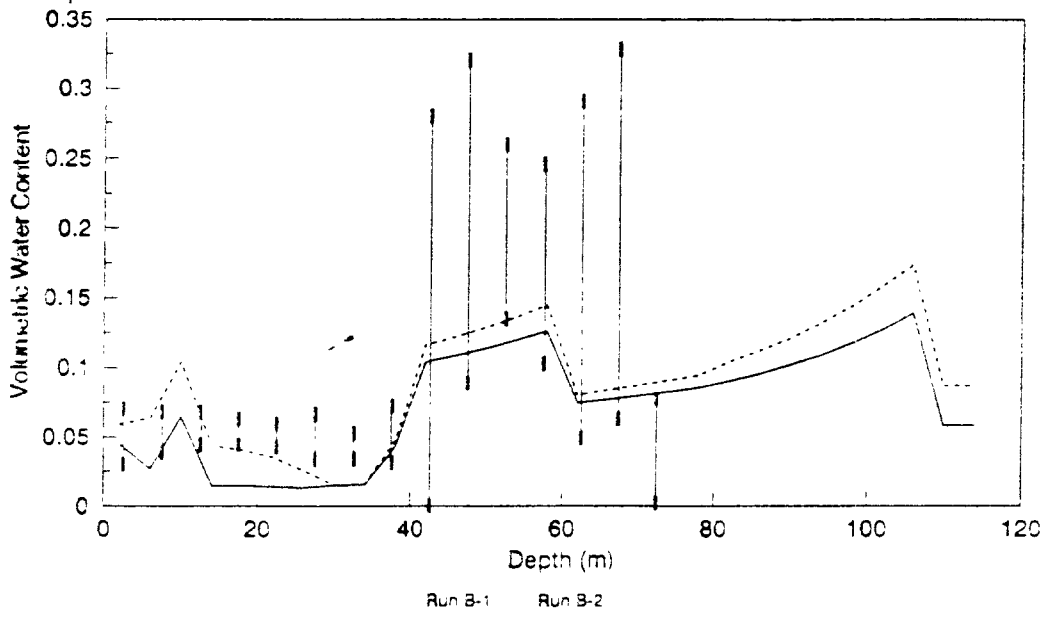


Figure 3. Pluvial infiltration models based on Spaulding (1983) for the 1 dimensional and fracture models. The infiltration signal shapes are based on 2 of Spaulding's interpretations of his data with magnitudes scaled to the conceptual models.

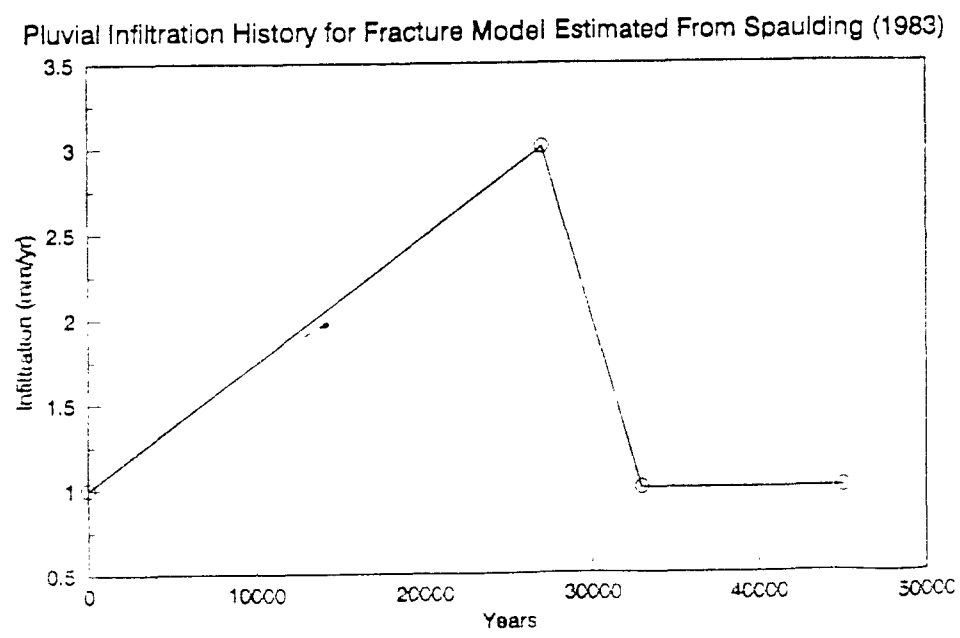
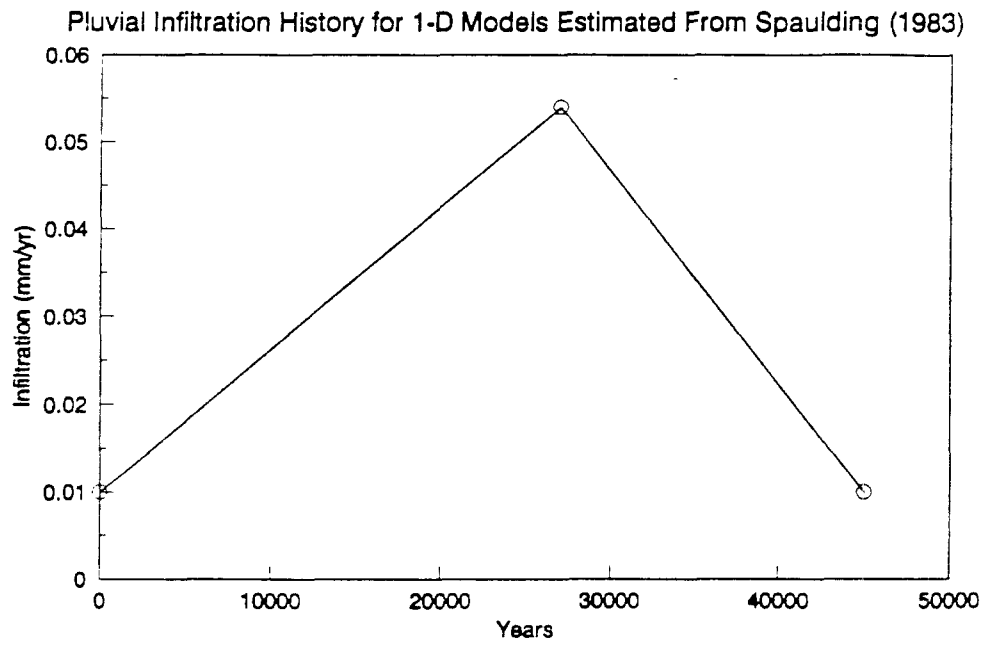
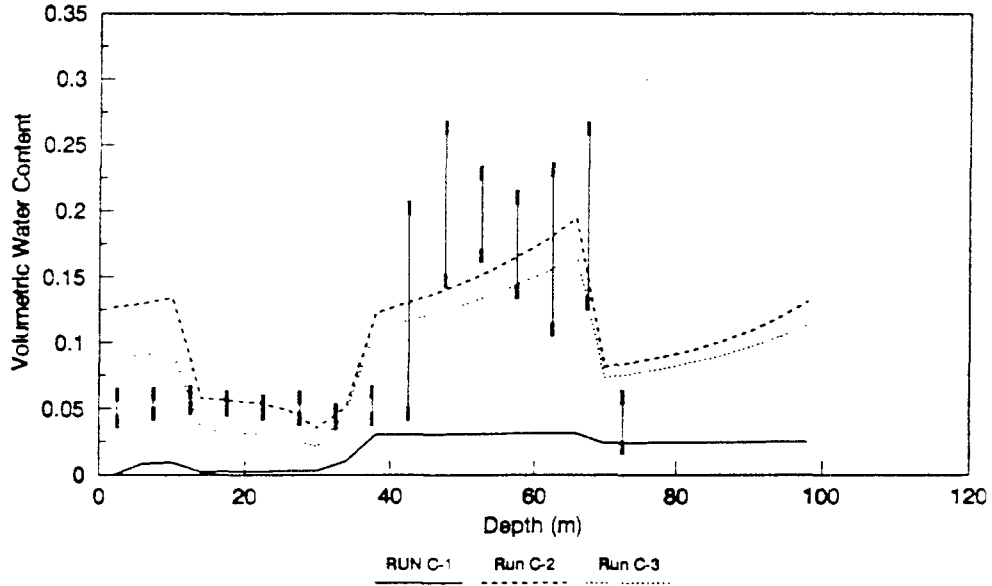
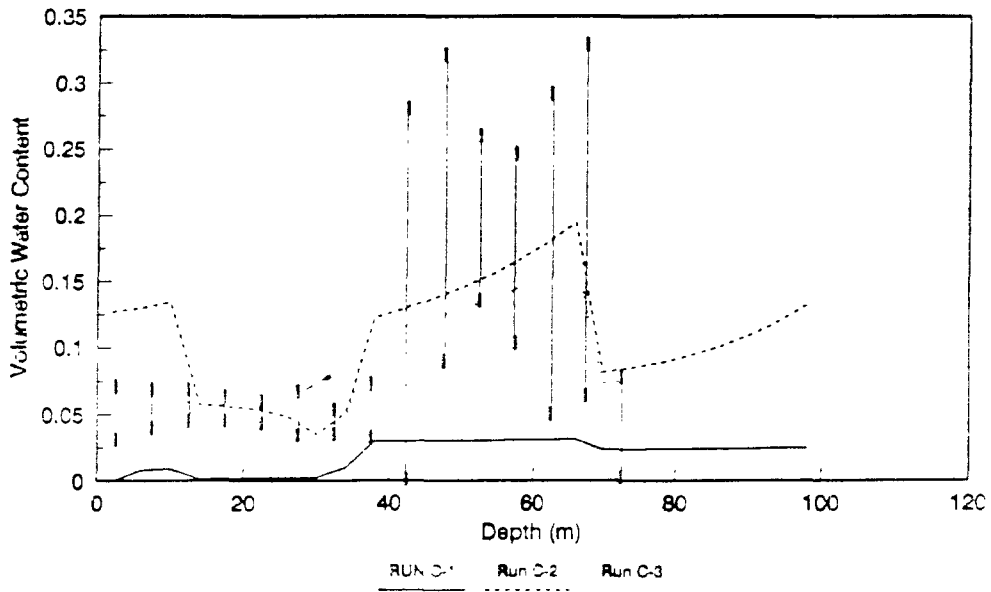


Figure 4. Comparison of simulated water contents using the 1-dimensional 7 unit runs with confidence intervals for working group data from shallow holes UZN-53, UZN-54 and UZN-55.

Comparison of Model with 68% Confidence Interval for Measurements



Comparison of Model with 95% Confidence Interval for Measurements



geometric mean plus 1 standard deviation, run C-2 used the geometric mean minus 1 standard deviation and run C-3 used the geometric mean. Three different infiltration scenarios were also used. For run C-1 an negative infiltration rate of -1.0 mm/yr was used. Run C-2 used steady infiltration of 0.0125 mm/yr and run C-3 used a "pluvial" infiltration history based on work done by Spaulding (1983). It is modeled starting 45,000 years ago with 0.01 mm/yr infiltration and increases linearly to a pluvial maximum at about 18,000 years ago with infiltration of 0.054 mm/yr and then decreases linearly back to 0.01 mm/yr at the present (Figure 3).

Run C-1 with 0 infiltration is much dryer than the measured data. Runs C-2 and C-3 appear similar. The transient infiltration signal for C-3 drops toward the present and this shows up in the modeled profile as a larger deviation from the steady infiltration induced curve of C-2, near the top of the column than at depth. In other words, the top of the column responds first to the dropping infiltration over time. Even at these near capacity infiltration rates, the modeled water contents are still low in the 40 to 70 meter range.

### Conclusions

Based on comparison of modeled water contents it is apparent that different combinations of conductivity models and infiltration scenarios may produce nearly identical water content profiles. The true difference between these simulations can only be examined by using a parameter with a time component. For example, runs A-1 and A-3 are virtually identical with respect to water content profile yet the vertical flux rate for A-1 is nearly 0 while for A-3 it is 0.01 mm/yr. Any model solution for water content alone will then be a non-unique solution in that other model configurations will yield the same result. Any model validation exercise should then include some criteria with a time domain component in order to bound flux or velocity estimates.

All of our 1-dimensional modeling did a poor job of matching the observed water content profiles and additional units did not improve the fit, in fact it seemed to deteriorate with the addition of more units. The relatively wet conditions measured within the upper high conductivity unit (40-70 meters depth), co-existing with the unsaturated conditions in the low conductivity units, such as the Upper Units and the Topopah below, could not be modeled with 1-dimensional geometry and infiltration realistically. The relationship between the water contents in adjacent units for a given infiltration rate is controlled by the water retention or characteristic curves which describe the nonlinear relationship between degree of saturation, capillary pressure and unsaturated conductivity. The higher retention properties in the unit at 40-70 meters causes water to be held at higher saturation in the unit above and below. This is due to the fact that at similar pressures the equilibrium saturation for this unit is much lower. Introducing a highly transient infiltration signal could theoretically produce the observed seemingly non-equilibrium relationships between the high conductivity zone and those adjacent. Due to the very low matrix conductivities however, it is nearly impossible to duplicate the saturation and water content relationships with any kind of realistic 1-dimensional infiltration scenario.

The model fit was also found to be relatively insensitive to changes in the matrix characteristic curves and conductivity models within the range of the supplied data. The discrepancy between the model and the data may be due to an over simplified conceptual model. The 1-dimensional, matrix dominated flow model may need to be expanded to include 2 or 3-dimensional effects such as lateral flow or flow within fractures that could produce the wet conditions in the area observed while allowing the unsaturated conditions observed in the Upper and Topopah Units. To explore this possibility we first tried a 2-dimensional model, then since we needed some estimate of the recharge mechanisms and amounts of recharge available to fractures and fault zones, we utilized a catchment area runoff model.

### **3. 2-Dimensional Model**

The finite element method was used to solve the 2-dimensional form of the Richards equation. The solution allowed for heterogeneous porous media conditions. A computer program implementing the finite element solution, called TWOD (Nieber et al., 1993) was applied in the analysis.

A 2-dimensional vertical section of the Yucca Mountain site was used. The vertical section was conceptualized to contain seven distinct porous media units (the same units as in the 7 unit, C series 1-D simulations presented in Table 2 and 3). The porous media properties in these units were represented by the van Genuchten equation for both the fluid retention and the hydraulic conductivity.

#### Model Geometry and Boundary Conditions

The vertical section was taken to be 750 meters wide and 488 meters deep with a water table as the lower boundary. The left vertical boundary was taken to be a faulted zone beneath the Solitario Canyon west of Yucca Mountain. A vertical line of symmetry was selected at a distance of 375 meters due east of this fault and a cross-section between these vertical boundaries modeled. Therefore we did not model the full 750 meters, but assumed symmetry on either side of the midline. The upper boundary of the matrix and fracture elements simulates atmospheric conditions. Gas pressure is fixed at 100,000 Pa and saturation near 0 for the entire simulation. The line of symmetry is taken to be an impermeable boundary. The finite element grid for the model domain consists of 720 nodes and 1330 linear triangular elements.

#### Initial Conditions And Infiltration History

The initial condition for all runs was assumed to be that of static equilibrium or no flow. Simulations were performed for times up to 200,000 years at which point the flow in the domain for all cases was at steady state.

It was assumed that water infiltrated at a mean rate of 0.1 mm/year through the top boundary of the region, while water infiltrated through the length of the fault boundary

on the west at two rates; 0.1 mm/year for run E-1 and 1.0 mm/year for run E-2. The source of water for the fault boundary is assumed to be water derived from recharge through the Ghost Dance Fault Zone and/or alluvium of the Solitario Canyon.

### Summary of Results

Two water content profiles are given in Figure 5, one for each of the fault flux rates. These profiles are for a vertical transect taken along the line of symmetry of the 2-dimensional domain. The 2-dimensional model results were similar to the 1-dimensional results. Conditions in Unit IV (Shardy Base, Non-Welded, Bedded Tuffs) were modeled consistently dryer than the data measurements. When higher infiltration rates were modeled areas of perched water appeared at the top of the Topopah and base of the Tiva Canyon Units.

Two-dimensional effects do not seem to be able to account for the relatively wet conditions measured in the high conductivity zone. Water movement laterally through the matrix is insufficient to significantly affect the water retention relationship between this unit and the unit above it. The high lateral input does cause elevated water contents in the base of the high conductivity unit and in the Topopah, immediately below.

Again it appeared a revised conceptual model was called for. The unsaturated zone conceptual model was expanded to include recharge that is focused by topography and areal surface material variation along with fracture flow. A mathematical model of water balance which could incorporate focusing mechanisms was also incorporated.

## **4. Depression Focused Recharge Model**

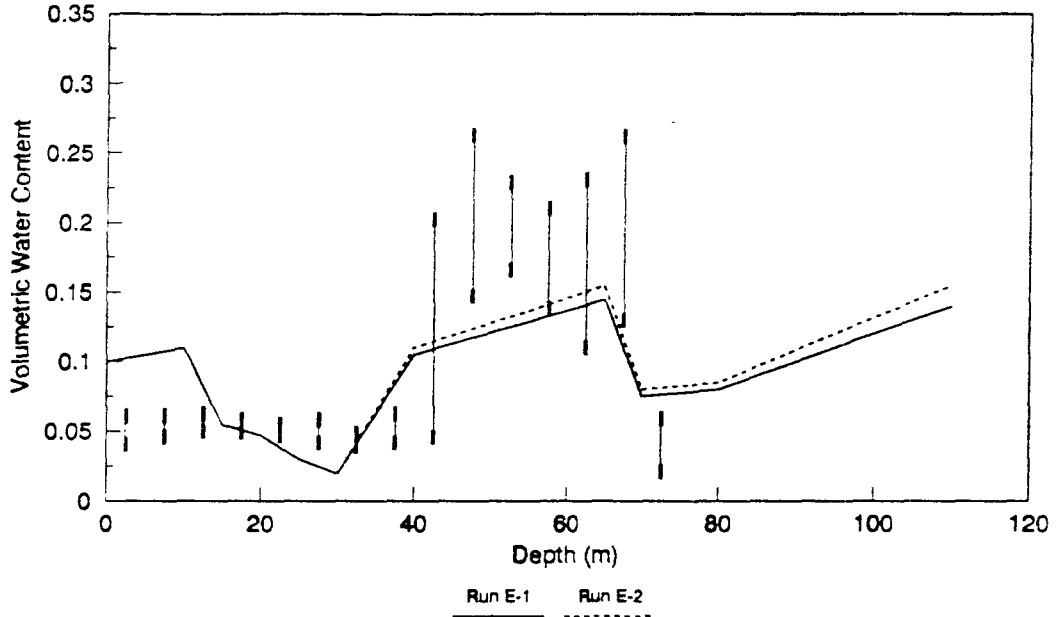
The Depression Focused Recharge (DFR) Model of Nieber et al (1993), was used to estimate recharge available to fractures and fault areas which lie near canyon or channel bottoms and are covered with alluvium.

The model performs a full water balance of the hydrologic cycle of a small catchment containing a topographic depression using stochastically generated weather variables, and determines the spatial and temporal structure of groundwater recharge. It considers the intensity and duration of rainfall for each rain event simulated, calculating runoff, evaporation and percolation for the catchment and depression. It takes into account the soil or rock hydrologic properties of the catchment and depression in calculating recharge as percolation which escapes evaporation.

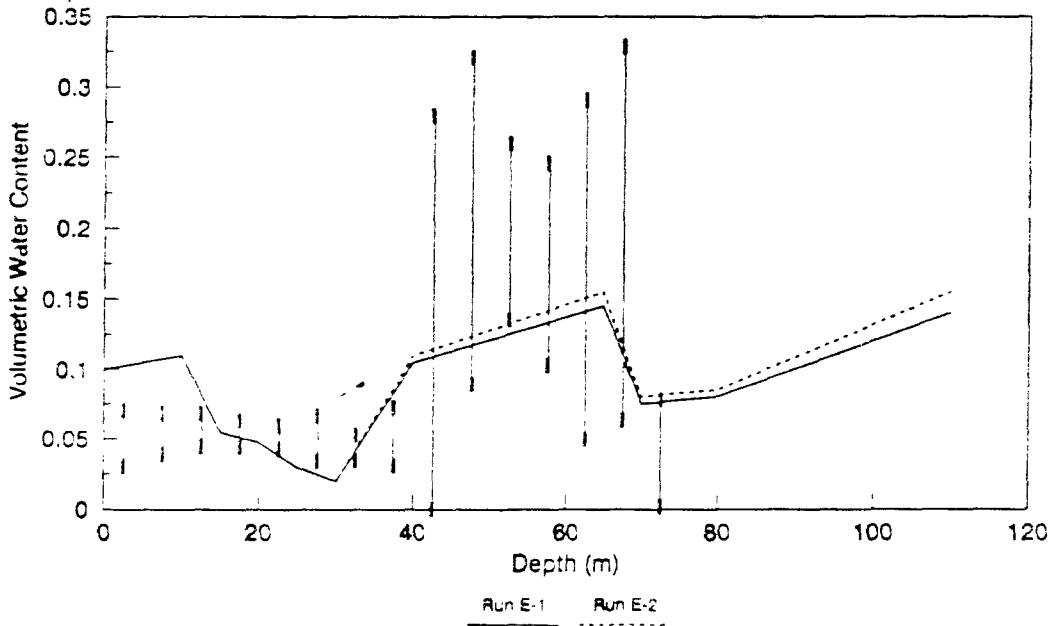
Weather data from the Tonopah, Nevada weather station was used to generate 20 years of rainfall and solar radiation using the CLIGEN model (Nicks, 1989). Precipitation at Tonopah averages approximately 130 mm/yr, slightly less than estimated for Yucca Mountain. The model generates climate conditions preserving the serial correlation of measured temperature, solar radiation and precipitation along with duration and

Figure 5. Comparison of 2-dimensional 7 unit runs with confidence intervals for working group data from shallow holes UZN-53, UZN-54 and UZN-55.

Comparison of Model with 68% Confidence Interval for Measurements



Comparison of Model with 95% Confidence Interval for Measurements



intensity statistics for precipitation events.

The 20 years of climate simulation was then used by the DFR model to perform a day by day cumulative mass balance of water entering and leaving the system. The model represents the catchment-depression system as a circular basin within which a depression with an outlet of fixed height exists (Figure 6). The climate simulation is applied uniformly over this circular geometry.

Two simulations were done using the geometry of the Solitario Canyon and two were done based on the geometry of the wash containing deep hole UZ-16. The catchment boundary was estimated from the topography and the depression was chosen as the area of low relief at the canyon bottoms. All simulations were run using the same climate data with the conductivity of the catchment based on the upper unit of the composite data and conductivity of the depression based on alluvium properties from Tyler (1985). The simulations were modeled as a single layer, with deterministic soil properties, and with outlet heights ranging from 0.01 mm to 100 mm. The outlet height represents a rough estimate of water depth in the depression bottom during a large precipitation event. Table 5 shows parameters used for the four runs. The runs were designed to give high and low estimates of recharge. The DFR model used corn plant characteristics to calculate transpiration and probably underestimates recharge slightly due to corn's short growing season and the lack of account for winter activity.

Run Solitario 1 used a lower value of conductivity for the catchment rock and a higher value of conductivity for the depression alluvium. Run Solitario 2 incorporated 1 mm of microdepression storage per rainfall event while run 1 had none. This resulted in a value of depression recharge 2.5 times higher for Solitario 1.

Run Hole Wash 1 used a lower value of conductivity for the catchment rock and a higher value of conductivity for the depression alluvium. For Hole Wash 1 an outlet height of 0.01 mm was used while Hole Wash 2 used a 10 mm outlet. Run Hole Wash 2 incorporated 1 mm of microdepression storage per rainfall event while run 1 had none. This resulted in a value of depression recharge 20 times higher for Hole Wash 2.

Figure 7 shows the model mass balance for the entire basin and for the depression, for model Solitario 2, the more conservative of the two Solitario runs with regard to recharge estimate. Each component of the model mass balance calculation is shown in the figure with evaporation representing total evaporation combined with transpiration. The total recharge in both simulations occurs only in the depression due to the relatively low conductivity of the "exposed" rock unit in the upper catchment. The amount of recharge for the runs totaled 12.1 cm/yr for run 2 and 30.8 cm/yr for run 1. The drill Hole Wash simulations found 8 mm/yr of recharge for run 1 and 16 cm/yr for run 2. These high recharge rates reflect the large proportion of runoff from the catchment rock and the high conductivity of the depression alluvium. This recharge is focused in the low alluviated area of the canyon, where fractures and faults are likely to exist

Table 5. Depression Focus Recharge Model Parameters and Result for Solitario Canyon and for Wash Where UZN-53, UZN-54 and UZN-55 are Located.

Properties	Solitario 1	Solitario 2	Hole Wash 1	Hole Wash 2
Catchment Area (m <sup>2</sup> )	6,157,500	6,157,500	1,242,324	1,242,324
Depression Area (m <sup>2</sup> )	1,131,000	1,131,000	253,388	253,388
Land Slope (deg)	5.7	5.7	5.7	5.7
Albedo	0.3	0.3	0.3	0.3
Outlet Height (m)	0.1	0.1	0.00001	0.01
Catchment Ksat (cm/s)	1.995E-8	1.089E-6	1.99E-7	1.99E-8
Catchment Porosity	0.15	0.15	0.15	0.15
Catchment Soil Storage Parameter (m)	0.099	0.099	0.099	0.099
Catchment Upper Limit of Stage I Evaporation (mm/day <sup>1/2</sup> )	5.2	5.2	5.2	5.2
Depression Ksat (cm/s)	4.0E-4	1.5E-4	4.0E-5	4.0E-4
Depression Porosity	0.51	0.51	0.51	0.51
Depression Soil Storage Parameter (m)	0.099	0.099	0.099	0.099
Depression Upper Limit of Stage I Evaporation (mm/day <sup>1/2</sup> )	5.2	5.2	5.2	5.2
Microdepression Storage (m)	0.0	0.001	0.0	0.001
Depression Recharge (m.yr)	0.308	0.121	0.008	0.160

Figure 6. Schematic of conceptual model for Depression Focused Recharge Model (Nieber et al., 1993)

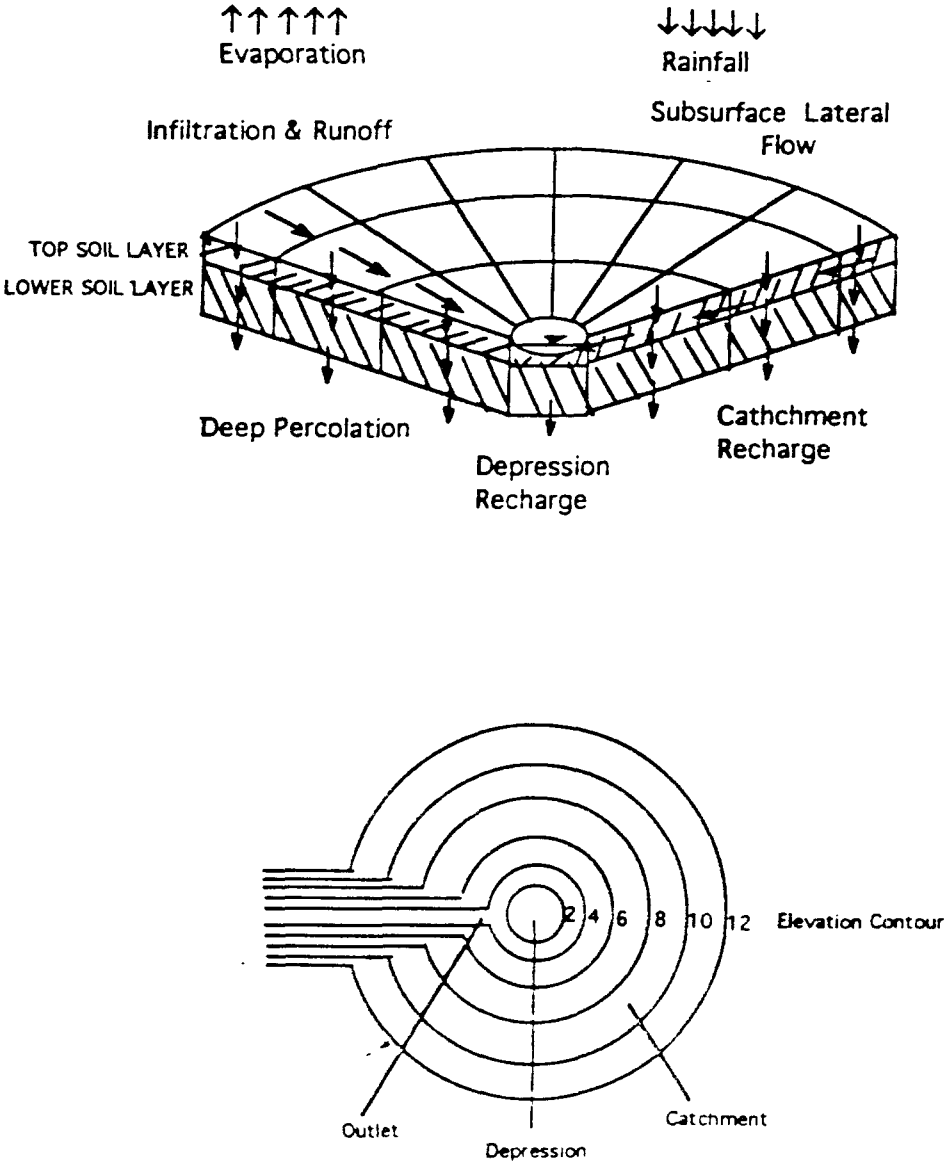
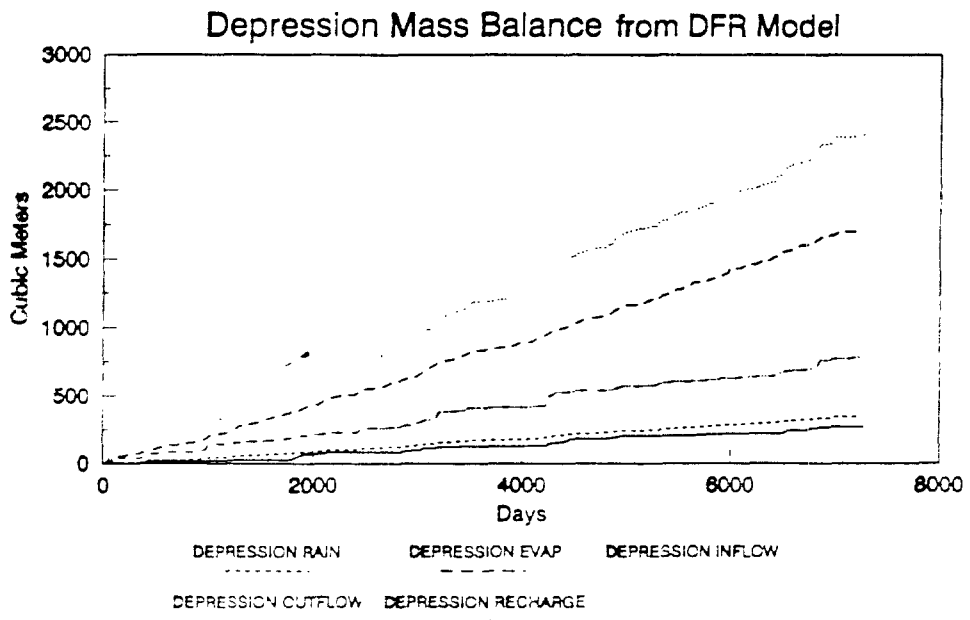
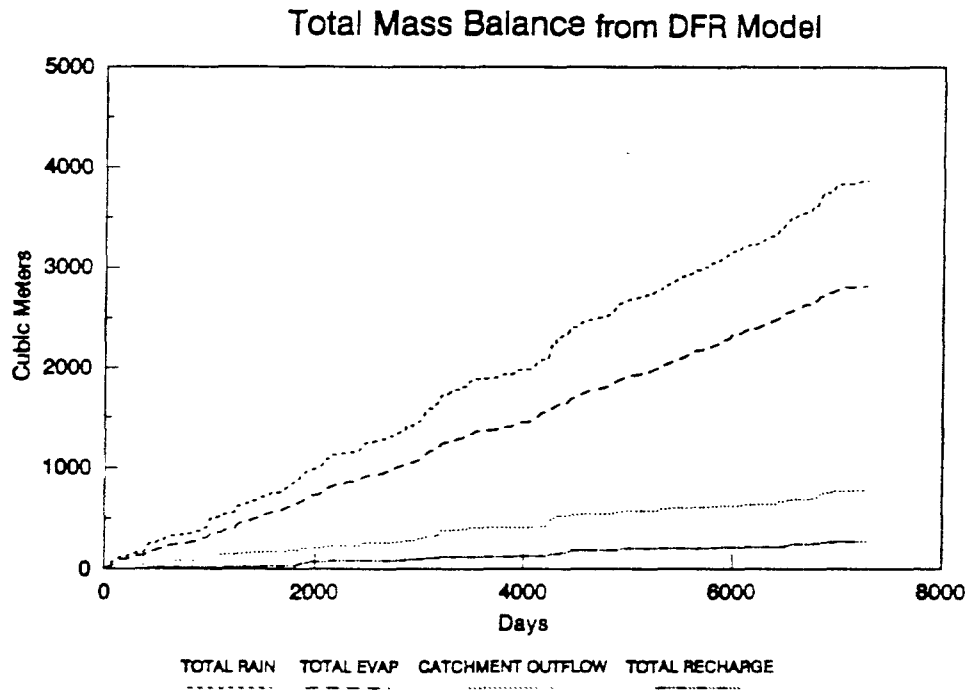


Figure 7. Plots of water mass balance for the Solitario Canyon simulation 2 simulated using the Depression Focused Recharge Model.



Recharge rates of 8 mm/yr to 300 mm/yr are considerably higher than estimates based on inverse 1-dimensional modeling and are specified for a particular morphology rather than a hypothetical uniform application. This is a much more realistic approach to estimating recharge on the site than the inverse modeling because it allows consideration of ground surface material, topography, and climate data. Hokett et al, (1991) have also shown that percolation rates at 1.2 meters depth of 5 cm could be achieved under simulated pluvial conditions in bare infiltration plots.

Using the recharge maps of Harrill et al. (1988) for Nevada, recharge water volume within the Yucca Mountain drainage was calculated by multiplying the map's estimated recharge by the area of the drainage. Then assuming this volume is focused into about 10% of the total area, near the ratio of valley bottom area to slope area, an estimated recharge of 6 mm/yr is obtained. This agrees well with our estimates based on the DFR model.

These high rates of recharge have not been previously utilized with our, or any other, unsaturated zone modeling efforts that have taken place for Yucca Mountain. If these estimates of potential recharge are within an order of magnitude of the actual recharge then either there must exist perched saturated zones within the alluvium filled canyons or a mechanism other than 1-dimensional or 2-dimensional matrix flow must prevail at the mountain. Since no perched saturated zones have been found in the alluvium adjacent to Yucca Mountain, it seems more likely that some mechanism of flow, such as fracture flow, is allowing recharge through the alluvium to percolate deeper. This supports our conclusion based on 1-dimensional modeling that an alternative conceptual model is appropriate. We therefore developed a fracture flow model based on a conceptual model that includes fracture dominated flow for the site.

## **5. Fracture Model**

One explanation for recharge rates higher than that allowed by the rock matrix, is that fracture flow plays an important role in the unsaturated zone at Yucca Mountain. To explore this possibility we have constructed a model which incorporates simplified fracture flow along with the composite data matrix properties.

The conceptual model upon which our fracture model is based can be outlined as follows. Yucca Mountain consists of four subhorizontal hydrologically distinct matrix zones with distinct properties as shown in Tables 4 and 5. This conception is based on our analysis of the working group data and is similar to the hydrological divisions used by Gauthier, et al. (1988). Three of the four units are significantly fractured while Unit 2 is not (Spengler and Chornack, 1984). The fracture surfaces are coated with minerals that reduce the conductivity between the matrix and fracture to 1/10 or less of the non-coated value (Thoma, et al., 1992). The fractures are vertically continuous in the units where they exist and are open to the atmosphere at the top and water table at the bottom of the column.

The water flux through the mountain is controlled by recharge, or infiltration, amounts and location. We assume rain water and snow melt generally runoff too rapidly to infiltrate much into the upper matrix unit and so tend to run into fractures open at the surface. Flow within fractures is initiated when input is higher than matrix conductivity. Water may also infiltrate areas of alluvium at canyon bottoms eventually reaching highly fractured fault zones below.

While there is a net inflow of water to the fractures, the upper matrix experiences net evaporation. This is due to the tendency of water to run off these tight rock units when it is available causing evaporation to dominate the mass balance of the upper matrix.

### Model Geometry

The geology of Yucca Mountain in the location of UZ-16 is simplified for our model and symmetry is utilized to minimize computation. Figure 8 shows the geometry of the dual porosity fracture model. The matrix stratigraphy is represented as a block of 4 hydrogeologic units. Except for Unit 2, the block is penetrated by regularly spaced vertical fractures. The fractures are spaced 3 per horizontal meter with average aperture of 200 microns (0.0002 m). The fracture conductivity is calculated based on the "cubic law" for flow within two parallel plates (Wang and Narasimhan, 1985). Because it is generally acknowledged that this calculation overestimates the actual conductivity, we used several apertures for calculation of the saturated conductivity to explore the range of possibilities (Table 8).

Three different characteristic curves for water retention were also used due to unavailability of measurements of these properties for fractures at Yucca Mountain. For these three Sandia Functions used to model fracture properties, the air entry value was varied from 600 Pa to 40,000 Pa while other parameters were held constant (Table 7). Figure 9 shows the three modeled fracture characteristic curves compared with the curve for matrix Unit 2.

The geometry is further simplified by utilizing symmetry of the simplified block. If symmetry is assumed, the block may be divided into identical matrix/fracture components and no flow boundaries used to "mirror" identical geometry. The actual modeled geometry is presented in Figure 8. The no flow boundary at left represents the centerline of an average matrix block, which is attached at the right to fracture elements. The fracture element is also bounded by a no flow boundary at its right. The width of the matrix elements then represents a characteristic matrix half length of 0.15 meters between 200 micron aperture fractures.

Fractures do not penetrate Unit 2 but are vertically connected to it. Horizontal fracture-matrix connection at Unit 1, Unit 3 and Unit 4 are reduced by 90% to simulate fracture coating inhibition of flow between fractures and surrounding matrix to 1/10 of their unrestricted value. One simulation was run with connection reduced by 99% to 1/100 the unrestricted value.

Figure 8. Schematic of conceptual geometry for dual porosity fracture model of unsaturated flow at Yucca Mountain simulated using VTOUGH computer code (Nitao, 1989).

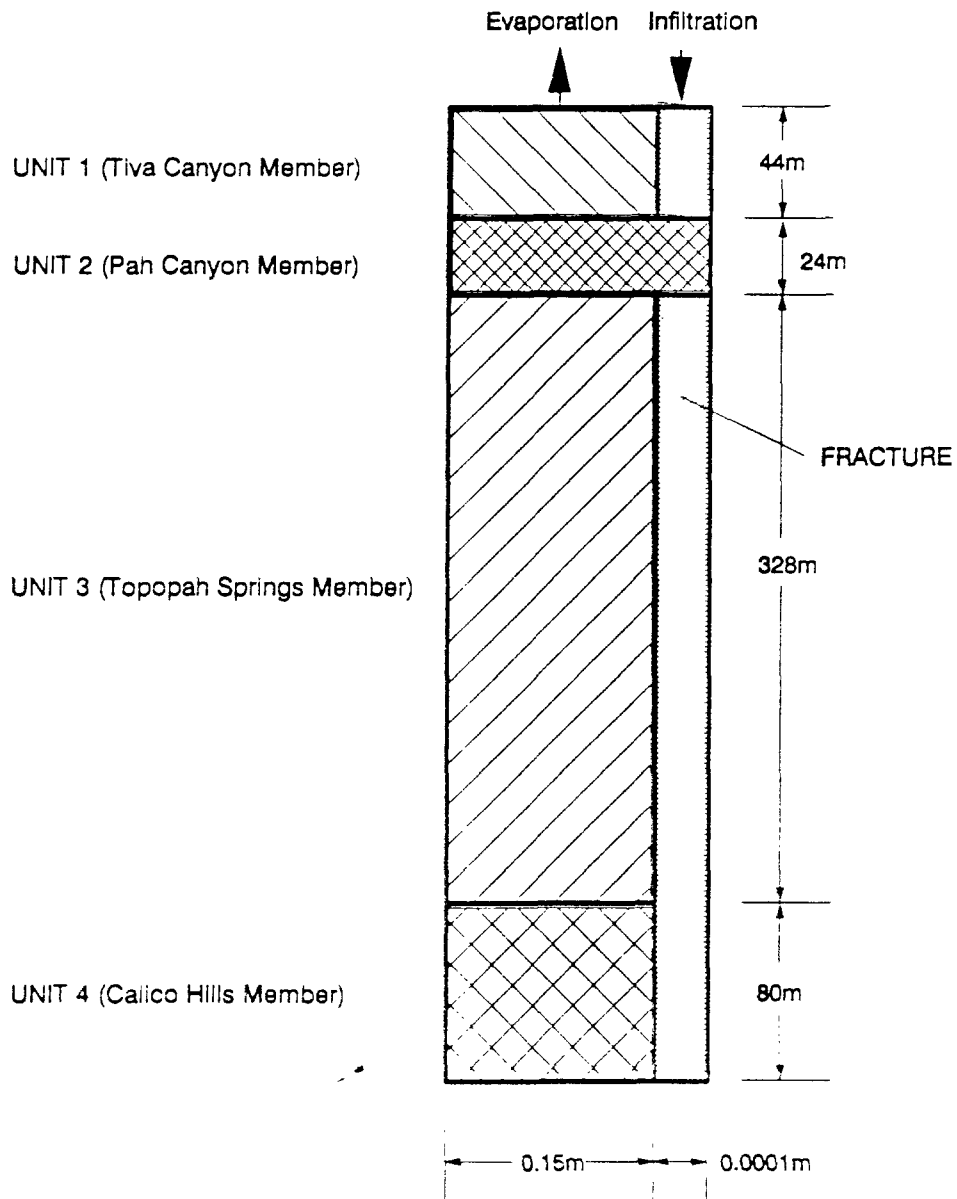


Table 6. Fracture Model Hydrologic Properties

UNIT	DEPTH INTERVAL (m)	$K_s$ (m/s)	POROSITY
1	0 - 44	5.25E-11	0.076
2	44 - 68	2.64E-6	0.388
3	68 - 396	6.18E-11	0.118
4	396 - 476	4.78E-11	0.240
FRAC A*	0 - 44 68 - 476	8.15E-3 - 0.130	0.990
FRAC B	0 - 44 68 - 476	8.15E-3 - 0.130	0.990
FRAC C	68 - 476	8.15E-3 - 0.130	0.990

Data from working group composite data and holes UZN-53, UZN-54 and UZN-55.

\* Fracture parameters based on Wang & Narasimhan (1985), and Spengler & Chornack (1984).

Table 7. Fracture Model VTOUGH Sandia Function Parameters.

UNIT	LAMBDA	$S_{lr}$	$S_{ls}$	$1/P_o$ (1/Pa)	$P_{max}$ (Pa)
1	0.21	0.04	1.0	1/130,000	5.0e+9
2	0.24	0.04	1.0	1/22,000	5.0e-9
3	0.24	0.04	1.0	1/150,000	5.0e+9
4	0.24	0.15	1.0	1/150,000	5.0e-9
FRAC A*	0.45	0.04	1.0	1/600	1.0e+9
FRAC B	0.45	0.04	1.0	1/30,000	1.0e+9
FRAC C	0.45	0.04	1.0	1/40,000	1.0e-9

Data from working group composite data and holes UZN-53, UZN-54 and UZN-55.

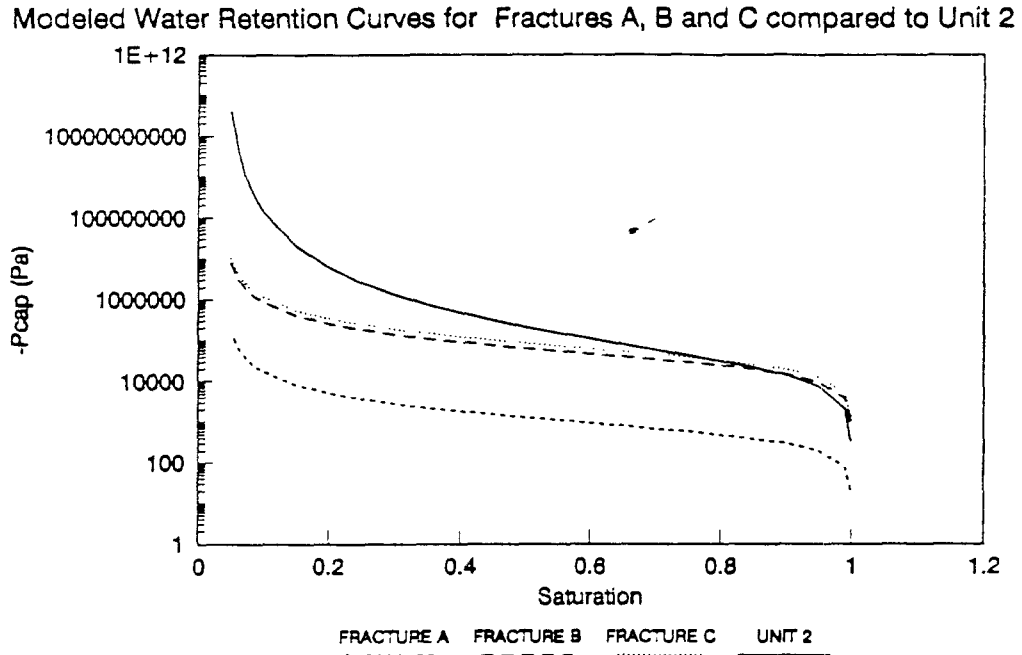
\* Fracture parameters based on Wang & Narasimhan (1985).

Table 8. Fracture Model Features for H Series Runs.

Run #	Infiltration History	Final Evaporation (mm/yr)	Fracture to Matrix Contact Area	Aperture for Conductivity ( $\mu\text{m}$ )	Fracture Water Retention Curve*
H-1	Pluvial	0.03	1/10	100	A
H-2	2 mm/yr	0.04	1/10	100	A
H-3	0.5 mm/yr	0.02	1/10	100	A
H-4	Pluvial	0.005	1/100	100	A
H-5	Pluvial	0.02	1/10	100	B
H-6	5 mm/yr	0.03	1/10	200	A
H-7	10 mm/yr	0.008	1/10	400	A
H-8	5 mm/yr	0.009	1/10	400 (upper) 300 (lower)	A (upper) C (lower)

\* See Figure 9.

Figure 9. Comparison of water retention curves for three modeled fractures with the characteristic curve for Unit 2 based on the measured data. Run H-5 used fracture curve B and run H-8 used curve C. The rest of the H series used fracture curve A.



The uppermost fracture element contains a water source which may be varied in time to simulate infiltration which changes in time. A water sink simulating net evaporation is placed in the uppermost Unit 1 matrix element. The model is set to extract as much for evaporation as is allowed by the available water in the upper matrix element and so varies between the fracture model simulations. Table 8 outlines the features of the 8 simulations runs.

### Boundary Conditions

The upper boundary of the matrix and fracture elements simulates atmospheric conditions. Gas pressure is fixed at 100,000 Pa (1 atm), and saturation near 0 for the entire simulation. The lower boundary of matrix and fracture elements simulate conditions at the water table. Pressure is fixed at 100,000 Pa and saturation at 1. The left and right domain boundaries are modeled as no flow boundaries.

## Initial Conditions And Infiltration History

The initial state of the model elements is that after 240,000 years without any water sources or sinks so that the column is nearly in equilibrium with the water table. Infiltration magnitudes have been varied from 1-10 millimeters consistent with estimates obtained from the DFR simulation. The "pluvial" infiltration history is based on work done by Spaulding (1983). It begins at 45,000 years ago and includes a pluvial maximum at about 18,000 years ago with infiltration of 3 mm/yr and a present minimum of 1 mm/yr. As previously mentioned, evaporation is modeled as a sink with potential maximum 0.1 mm/yr but which is limited by water available within the matrix element.

## Summary of Results

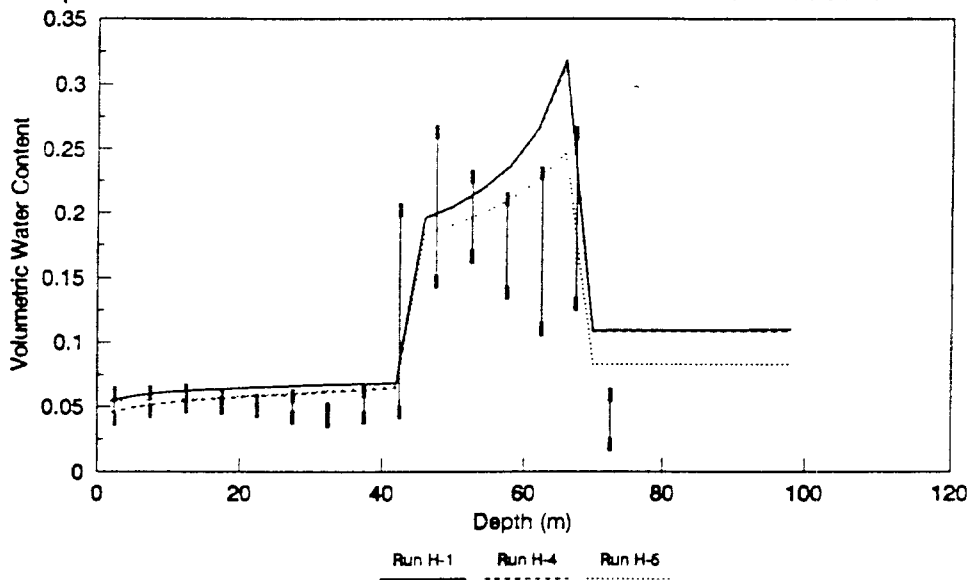
The results of the 4 unit, fracture simulations are shown in Figures 10 through 12. The modeled water content profiles are plotted versus depth and compared to measured data confidence intervals. The measured water content confidence intervals are found in the same manner described in Section 1, by grouping the data to include all measurements found in each 5 meter span. The modeled water content profiles are taken from the matrix elements of the model. The matrix water content profiles are emphasized because this quantity is actually measured at the boreholes and this was chosen as the calibration measure by the INTRAVAL working group. Simulated water content profiles are shown nearly at steady state except for the runs using the pluvial infiltration signal which covers 45,000 years then terminates.

Simulation runs H-1, H-4 and H-5 are shown in Figure 10. All use the pluvial infiltration signal (Figure 3). Run H-4 has fracture/matrix contact area reduced to 1/100. This reduced transmissivity between elements is used to simulate the effects of fracture coating. Run H-5 uses a characteristic curve with air entry value 30,000 Pa rather than 600 Pa (Fracture B, Figure 9). This curve is somewhat midway between the original fracture curve and the matrix curves.

The upper 40 meters or so of the measured water content profiles are matched well and the high conductivity matrix unit from 40 meters to about 70 meters is also reasonably well duplicated except for the high modeled water contents near the base of this unit. These high modeled values are due to the high saturation needed in the matrix elements to initiate flow in the fracture and allow water to continue downward from unit 3 at the input rate. Run H-5 with fracture characteristics closer to the matrix properties shows improved agreement with the data. The very high saturations in the base of the high conductivity unit and within the Topopah below, modeled in H-1 and H-4, are significantly lower in H-5. H-5 maintained the good match with the upper profile data and brought the lower part of the profile into the measured range. The physical basis for this characteristic curve is the possibility of fracture filling clays and coatings which increase the air entry value for the fractures.

Figure 10. Comparison of water contents modeled in matrix elements for runs H-1, H-4 and H-5 using the dual porosity fracture model with confidence intervals for working group data from shallow holes UZN-53, UZN-54 and UZN-55.

Comparison of Model with 68% Confidence Interval for Measurements



Comparison of Model with 95% Confidence Interval for Measurements

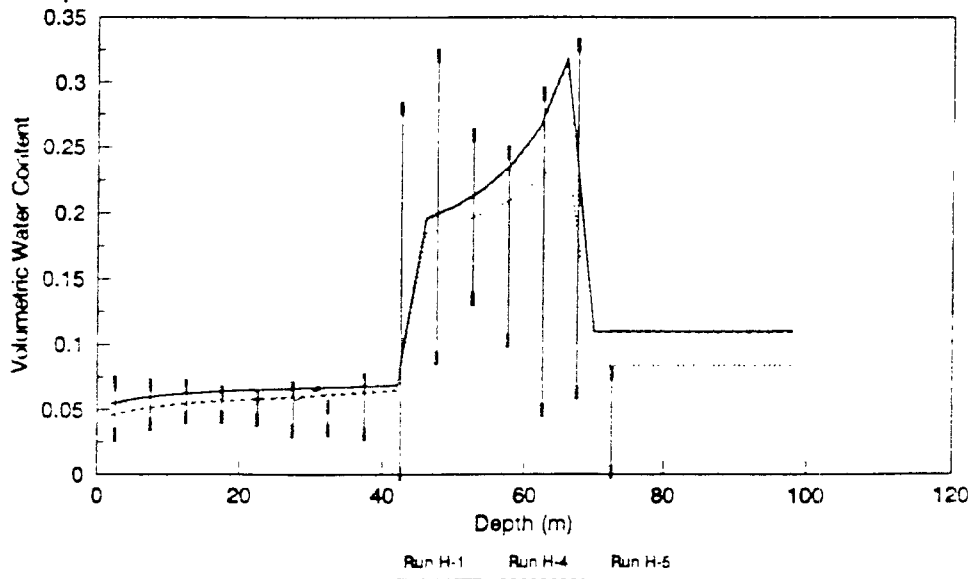
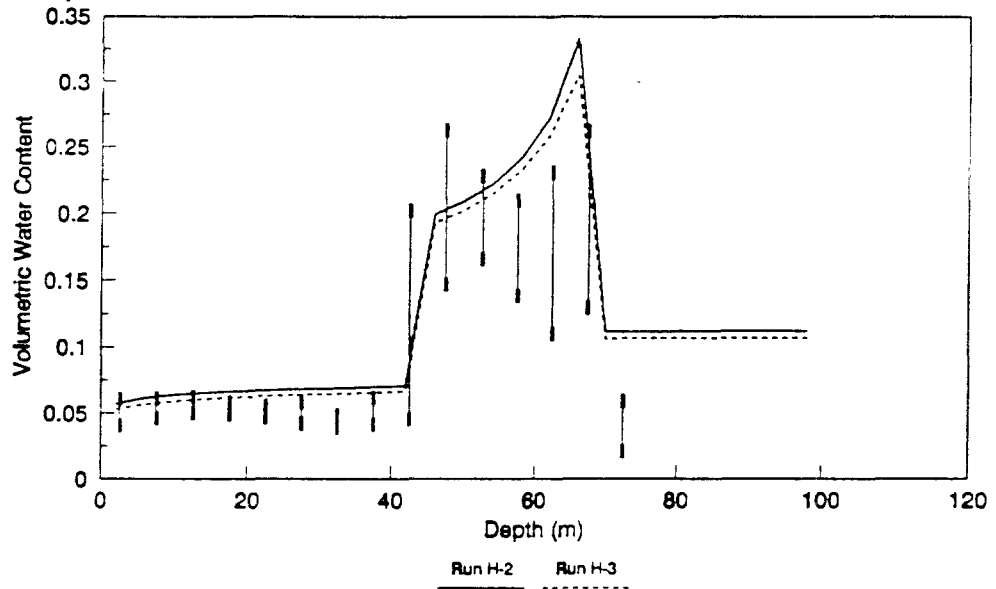
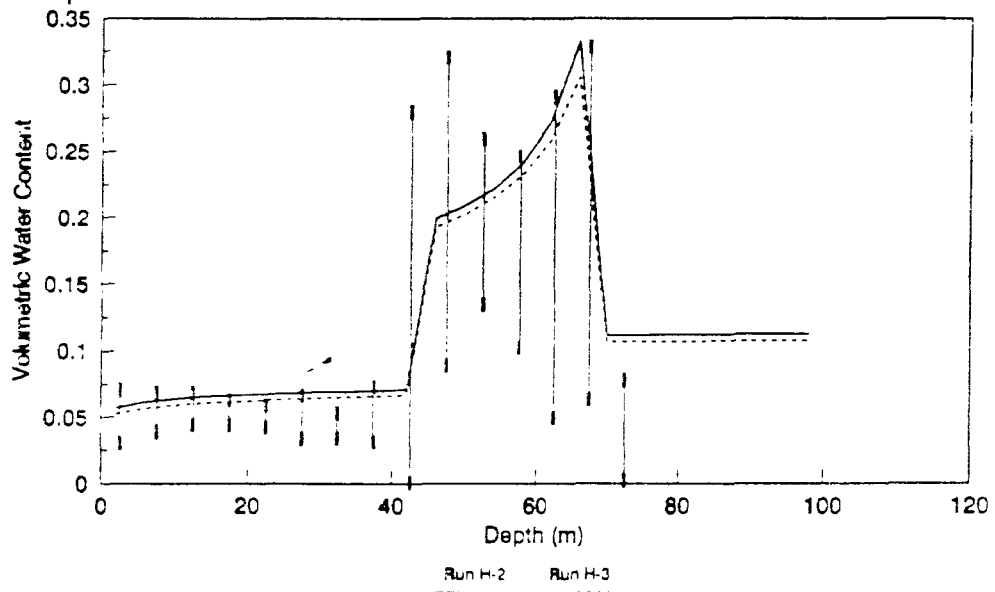


Figure 11. Comparison of water contents modeled in matrix elements for runs H-2 and H-3 using the dual porosity fracture model with confidence intervals for working group data from shallow holes UZN-53, UZN-54 and UZN-55.

Comparison of Model with 68% Confidence Interval for Measurements



Comparison of Model with 95% Confidence Interval for Measurements



The effect of reducing the fracture/matrix area by a factor of ten in run H-4 produced no noticeable effect on the modeled profile. This is probably due to the long time period of the simulations, about 45,000 yrs. Over this time span the matrix elements and fracture elements come to near equilibrium and so the effect of reducing fracture/matrix connection area for this model is seen in modeled profiles only after short time periods.

The matrix elements take longer to wet but after enough time they reach the same levels as with the higher contact transmissivity. This points out a shortcoming of this modeling exercise. We have not been able to model individual infiltration events over the time required, and so we look at yearly averages in infiltration. This means that conditions in the modeled fracture reach a sort of steady state and the full effect of fracture matrix interaction in real time is lost. Water content profiles are then properly seen as yearly averages themselves.

Simulations H-2 and H-3 are shown in Figure 11. Run H-2 has a steady state infiltration four times H-3 but is otherwise identical. These results are similar to runs H-1 and H-4. The high conductivity unit between 40 and 70 (Unit 2) meters, as well as the Topopah below, are too wet. Again, the relationship between the water retention properties of the fracture and those of Unit 2 dominate the saturation modeled in Unit 2. Varying the infiltration by a factor of 4 had little effect.

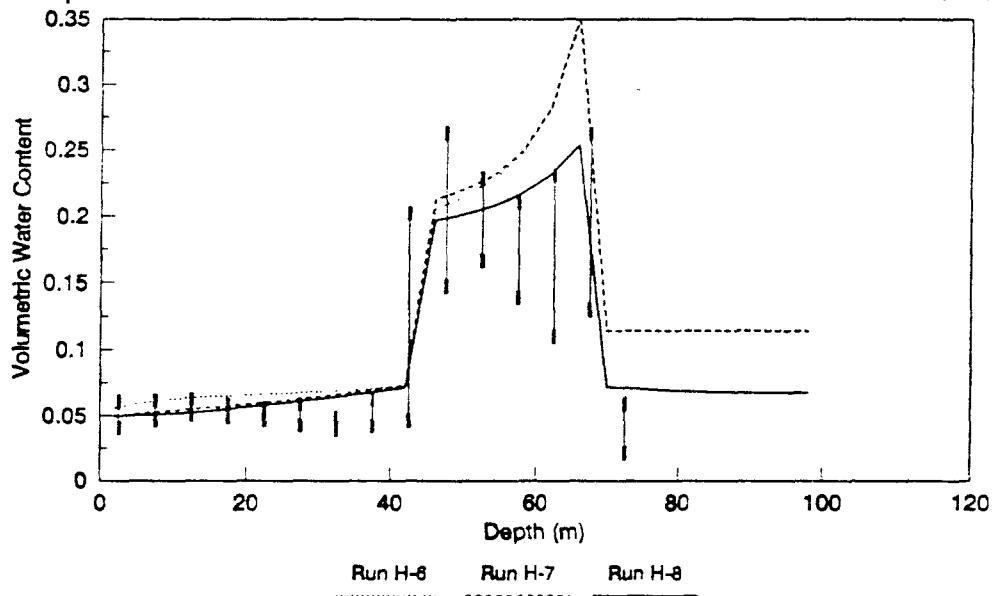
Simulations H-6, H-7, and H-8 are presented in Figure 12. Runs H-6 and H-7 return to the model configuration of H-1 except that larger fracture apertures were used for the geometry and conductivity calculation. The modeled water content profiles for H-6 and H-7 were somewhat wetter near 60 meters but otherwise similar to those of runs H-1 through H-4 while allowing infiltration rates 5-10 times higher.

Simulation H-8 combines higher fracture apertures with distinct characteristic curves for the upper fracture, above 40m, and the lower fracture, below 70m. Water retention for the lower fracture is modeled with a higher air entry value which makes it more like the matrix than the upper fracture. This will cause the lower fracture to hold more water at higher capillary suction than the upper fracture. This configuration was based on observation of the previous modeled profiles compared to the measured data and the effects of changes in the input parameters. This modeled profile seems to fit the data better than any of the other models we have assembled. The physical basis for assuming distinct water retention curves for fractures in the upper unit and the lower units lies in the likelihood that fractures within these units probably have different densities, amounts of fillings, surface roughness, and aperture distributions all of which will effect the unsaturated properties.

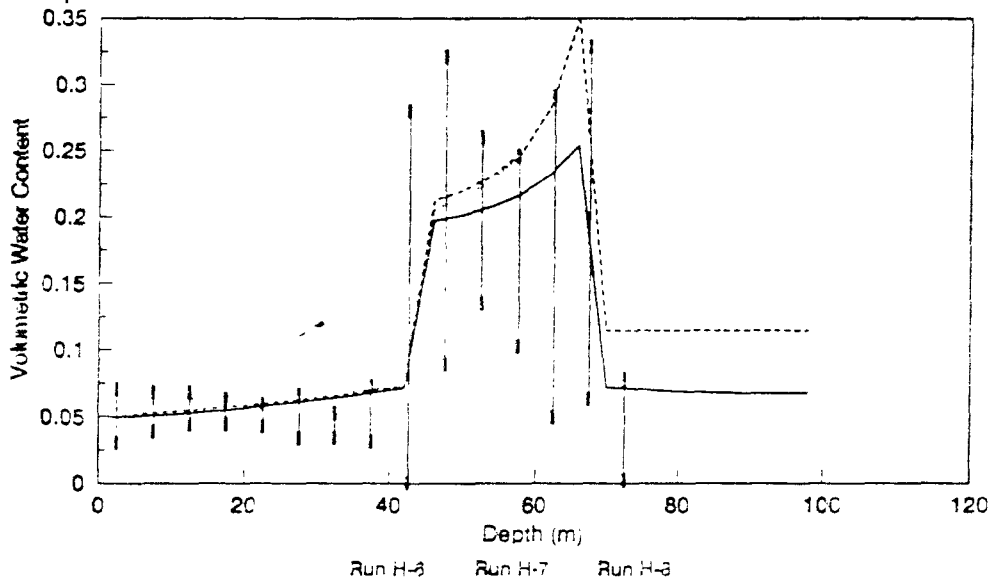
The fracture models show that the high saturation existing in the area of Unit 2 may be explained by infiltration greater than the matrix will allow. This flow arrives through fractures in the highly fractured units above. It causes storage in the relatively unfractured Unit 2 until it is wet enough to allow the flow to continue down the fractures below. The relationship between the fracture and matrix hydrologic properties is crucial to this analysis. Much good matrix data are available but information on

Figure 12. Comparison of water contents modeled in matrix elements for runs H-6, H-7 and H-8 using the dual porosity fracture model with confidence intervals for working group data from shallow holes UZN-53, UZN-54 and UZN-55.

Comparison of Model with 68% Confidence Interval for Measurements



Comparison of Model with 95% Confidence Interval for Measurements



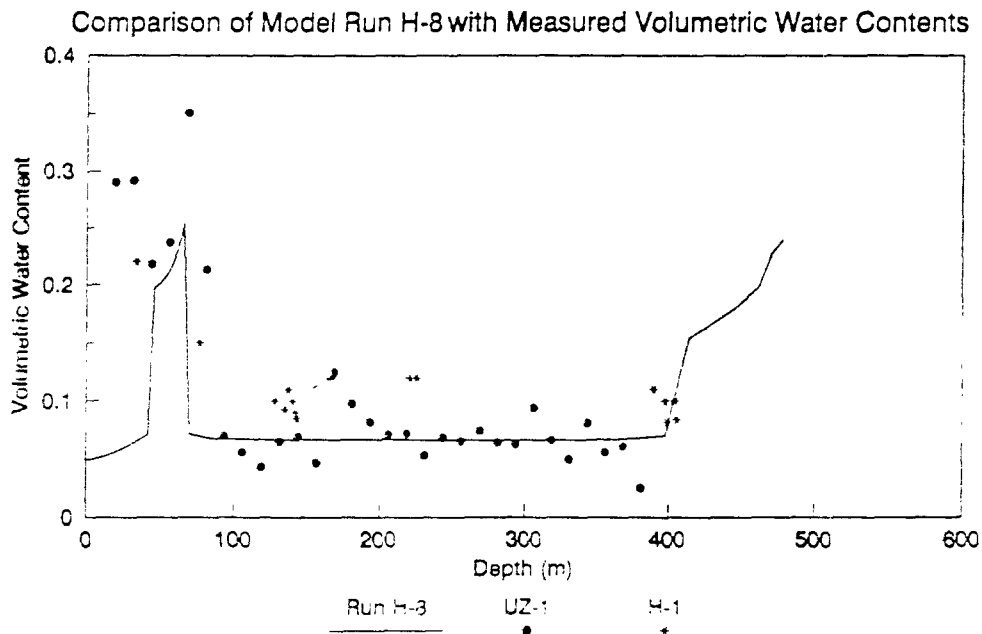
fracture properties is limited and so assumptions were made regarding them in this study.

As with the 1-dimensional models, the fracture models show that nearly identical water content profiles may be obtained using models with a wide range of infiltration amounts and hydrologic property assumptions. It is also possible to simulate good matches to the water content data by using infiltration on the order of centimeters/year and stopping the simulation at 500 to 1000 years before water contents reach equilibrium and become too high. The important differences in these apparently similar solutions would be obvious when flow rates or velocities are examined.

The water content data can be reasonably simulated by using different combinations of infiltration and conductivity as well as different combinations of infiltration and total simulation time. For that reason validation of the fracture model cannot be reliably done without additional criteria with a time component.

A limited amount of data from deeper drill holes is available. To examine the accuracy of our best model at levels deeper than 100 meters, Run H-8 was compared with data from deep holes USW UZ-1 (Whitfield et al., 1990) and USW H-1 (Rush et al., 1983). Figure 13 shows Run H-8 compared with individual measurements for USW H-1 and with measurements averaged over 15 meter intervals for USW UZ-1. The stratigraphy

Figure 13. Comparison of deep hole data with simulation Run H-8.



within the upper units is only loosely correlated between these two holes and the shallow drill holes UZN-53, UZN-54 and UZN-55 modeled but correlation of the Topopah Springs Unit below 100 meters is very good. Significant variation between these two holes is also evident. The fact that USW H-1 was wet drilled while USW UZ-1 was dry drilled may account for some of the difference. Differences in geology probably plays a major role as the two measured profiles cross near the 100 meter mark where USW H-1 changes from the dryer profile to the wetter of the two. This may indicate that significant horizontal variation of hydrologic properties exist within the Yucca Mountain units so that unsaturated zone models will have to account for this complexity if a site-wide model is desired.

It can be seen that Run H-8 falls within the water content data below 100 meters for these holes. Water contents within the upper units above 100 meters is not as good. This discrepancy may be due to differing stratigraphy between the model and hole locations as well as different morphological surface conditions between those assumed for the model and existing at the deep holes.

## **6. Summary and Conclusions**

The most sensitive parameters for this model of Yucca Mountain unsaturated flow are the fracture unsaturated conductivity curves and water retention characteristics as well as the rates of past and present infiltration. These determine the amount of yearly averaged input to the system and the degree of wetting in the model elements it causes. Unfortunately these are probably the least understood of the hydrologic properties measured thus far at the Yucca Mountain site. We have found though, that the water content profiles we have simulated using this fracture model are not extremely sensitive to infiltration magnitudes or functional shape of the infiltration signal. Values below about 1 millimeter cause simulations that appear too dry and those above 10 or so millimeters appear too wet. But, varying the infiltration magnitudes in the range of 1 to 10 millimeters serves mainly to fine tune certain aspects of the modeled profile rather than cause large scale changes in the profile shape or magnitudes. This robustness of the modeled water content profile with regard to the infiltration signal is advantageous considering the large uncertainty in, and transient nature of, the actual infiltration signal.

At the time scales we are able to examine using this model, fracture coating has little impact on modeled water content and at 10,000-50,000 years, depending on the degree of flow inhibition between fracture and matrix, a near steady state flow condition is achieved. Variation in matrix properties within the range of measurements seem to have small effect on the modeled water contents.

We have found for this case that increasing the number of hydrologic units modeled decreases the accuracy of the model. Too many units caused the water content profile to begin to exhibit the variation in the measurements due to measurement error and natural random variation within a representative elementary volume (REV). This is to

be expected when the number of data points upon which a differentiated unit is based becomes too small to be a representative sample, increasing the sample mean variance. Four units seem here to capture the detail needed to model the water content profile without adding spurious detail.

Our estimates of infiltration for the Yucca Mountain site based on our own modeling using the DFR model of Nieber et al. (1993), and estimates of others, including Harrill et al. (1988) and Hokett et al. (1991), have been consistently much higher than the maximum that matrix flow alone will allow here. Considering the process of fracture flow allows these higher infiltration rates while maintaining agreement between water content data collected and modeled water contents. Based on this study, the conceptual model for unsaturated flow at Yucca Mountain becomes more accurate with the addition of fracture flow and focused infiltration to the stratified matrix system commonly accepted.

While we feel we have accounted for the important flow mechanisms operating at Yucca Mountain, the primary measure of model accuracy will ultimately be the degree of agreement with actual data collected. We feel that at present the data available to rate the accuracy of our model is too limited. We have seen that different combinations of model input lead to nearly identical modeled water content output not revealing important differences between them. Comparing the modeled water content only, can not validate the model or provide a rigorous yardstick to evaluate the model's accuracy. Some data in the time domain such as chemical data or accurate infiltration measurements are needed to properly constrain this modeling problem and avoid non-unique solutions.

## REFERENCES:

Gauthier, John H., Nalini B. Zieman, and Warren B. Miller, TOSPAC calculations in support of the COVE 2A benchmarking activity, SAND88-2730 • UC-814, October, 1991.

Harrill, J.R., Gates, J.S., and Thomas, J.M., Major ground-water flow systems in the great basin region of Nevada, Utah, and adjacent states, USGS Atlas HA-674-C, 1988.

Hokett, S.L., G.F. Cochran, and S.D. Smith, Shallow vadose zone response to a simulated pluvial climate at a field site near Yucca Mountain, Nevada, Submitted for publication in the "Special Issue of Radioactive Waste Management and the Nuclear Fuel Cycle on the Yucca Mountain Project", 1991.

Lehman, Linda L., Alternate conceptual model of ground water flow at Yucca Mountain. Proceedings of High Level Radioactive Waste Management, April 12-16, 1992.

Montazer P., and Wilson, W.E., Conceptual hydrologic model of flow in the unsaturated zone, Yucca Mountain, Nevada, USGS Water-Resources Investigation Report 84-4345, 1984.

Nicks, Arlin, CLIGEN version 1.0, WEPP Water Erosion Project, Durant OK, 1989.

Nieber, J.L., Munir, H., and Friedel, M. A finite element model of unsaturated flow using simplex elements, US Bureau of Mines, 1993.

Nieber, J.L., Tosomeen, C.A.S., and B.N. Wilson, A stochastic-mechanistic model of depression focused recharge, Second USA/CIS (formerly USSR) Conference on Environmental Geology and Hydrology, Washington D.C., May 15-21, 1993.

Nitao, J.J., V-TOUGH--An enhanced version of the TOUGH code for the thermal and hydrologic simulation of large scale problems in nuclear waste isolation, Rep. UCID-21954, Lawrence Livermore Natl. Lab., Livermore Calif., 1989.

Pruess, K., 1987, Tough user's guide, Sandia National Laboratories and Division of Waste Management Office of Nuclear Material Safety and Safeguards, U.S. Nuclear Regulatory Commission, NUREG/CR-4645, SAND 86-7104 RW.

Rush, F.E., Thordarson, W. and Bruckheimer, L., Geohydrologic and Drill-Hole Data for Test Well USW H-1, Adjacent to Nevada Test Site, Nye County Nevada, USGS Open-File Report 83-141, 1983.

Spaulding, G. W., Vegetation and climates of the last 45,000 years in the vicinity of the Nevada Test Site, South-Central Nevada, USGS Open-File Report 83-535, 1983.

Spengler, R.W., and M.P. Chornack, Stratigraphic and structural characteristics of volcanic rocks in core hole USW C-4, Yucca Mountain, Nevada, Nye County, Nevada, USGS Open-File Report 84-789, 1984.

Thoma, Steven G., David P. Gallegos, and Douglas M. Smith, Impact of fracture coatings on fracture/matrix flow interactions in unsaturated, porous media, Water Resources Research, Vol. 28, No. 5, pp 1357-1367, May, 1992.

Tyler, S.W., Review of Soil Moisture Flux Studies at the Nevada Test Site, Nye County, Nevada, Water Resources Center Desert Research Institute: University of Nevada, Publication #45058, 1987.

Wang, J.S.Y., and T.N. Narasimhan, Hydrologic mechanisms governing fluid flow in a partially saturated, fractured, porous medium, Water Resour. Res., Vol. 21, No. 12, pp 1861-1874, Dec., 1985.

Whitfield, M.S., Thordarson, W. and Hammermeister, D.P., Drilling and Geohydrologic Data for Test Hole USW UZ-1, Yucca Mountain, Nye County, Nevada, USGS Open-File Report 90-354, 1990.